Supporting information for:

Zinc complexes of $Ttz^{R,Me}$ with O and S donors reveal differences between Tp and Ttz ligands: acid stability and binding to H or an additional metal ($Ttz^{R,Me}$ = tris(3-R-5-methyl-1,2,4-triazolyl)borate; R = Ph, *t*Bu)

Mukesh Kumar,[a] Elizabeth T. Papish,*[a] Matthias Zeller[b] and Allen D. Hunter

[a]*Department of Chemistry, Drexel University, 3141 Chestnut St.,*

Philadelphia, PA 19104, USA. E-mail: elizabeth.papish@drexel.edu

[b]*Department of Chemistry,Youngstown State University, 1 University Plaza,*

Youngstown, OH 44555

Single crystal X-ray diffraction data In **2** the CH_2-CF_3 moiety is disordered over two positions in a ratio of 0.8869(17) to 0.1131(17). Equivalent bond distances in the two disordered sections were restrained to be similar and ADPs structure with a total volume of 3319 cubic Angstrom (12.4% of the unit cell volume). These voids are most likely filled with several hexane molecules since this was the recrystallization solvent and no impurities were seen in the NMR spectra of **3** prior to recrystallization. The positions of the solvent molecules are however not well defined and no satisfying solvent model could be developed. The electron density within in the voids was thus corrected for using the SQUEEZE procedure[1] implemented in Platon[2] (see squeeze report appended to the cif file). In **5** the phenol solvate molecule is located on a crystallographic inversion center and the OH group is disordered with the *para* H atom in a 1:1 ratio. In **7** the crystal under investigation was found to be non-merohedrally twinned. The orientation matrices for the two components were identified using the program Cell Now,[3] and the two components were integrated using Apex2, resulting in a total of 22947 reflections. 9546 reflections (7096 unique) involved component 1 only (mean $I/\sigma = 13.9$), 9436 reflections (6937

unique) involved component 2 only (mean I/σ = 3.8), and 3961 reflections (3682 unique) involved both components (mean I/σ = 13.1). 4 reflections (4 unique) involved 3 domains (mean I/σ 5.3). The exact twin matrix identified by the integration program was found to be 0.99810 0.01028 -0.02859, 0.03667 -0.99969 0.01328, -0.11929 -0.01762 -0.99818. The data were corrected for absorption using Twinabs,[4] and the structure was solved using direct methods with only the non-overlapping reflections of component 1. The structure was refined using the hklf 5 routine with all reflections of component 1 (including the overlapping ones) below a d-spacing threshold of 0.75 Å, resulting in a BASF value of 0.085(1). No racemic twinning was observed. The R_{int} value given is for all reflections before the cutoff at d = 0.75 Å and is based on agreement between observed single and composite intensities and those calculated from refined unique intensities and twin fractions. In **8** the structure exhibits pseudo-monoclinic symmetry and the crystal at hand was found to be pseudo-merohedrally twinned by this symmetry. The structure was refined under application of the twin law 1 0 0, 0 -1 0, 0 0 -1 using the hklf 4 routine and the twin ratio refined to 0.4944(9) vs 0.5056(9). The pseudo-symmetry is both metric with two unit cell angles very close to 90 degrees, as well as internal. The two crystallographically independent molecules are related by a pseudo glide plane (in the setting used an n-glide plane passing through 0.252 0 0 and 0 0.5 0.5) which would convert the space group into $P2_1/n$ after resorting of the cell axes. The maximum deviation for non-fitting atoms for this pseudo glide plane is between 0.35 and 0.45 Å.[5] Systematic absences for the glide plane (and the associated 2_1 screw axis) are clearly not obeyed. Attempts to refine the structure in a monoclinic setting in $P2_1/n$ results in disorder of two of the phenyl rings in the then single independent molecule, but even under consideration of disorder R values are persistently high with R1 being ca 13-14%. Thermal parameters of the disordered atoms are not clearly defined

with some being non-positive definite and residual electron densities are high. In $\mathbf{10_{H2O}}$ one of the two solvate benzene molecules is located on a crystallographic inversion center. It shows large thermal motion and was refined as slightly offset from this center and constrained to resemble an ideal hexagon with C-C distances of 1.39 Å. Opposite carbon atoms were constrained to have identical ADPs and all disordered C atoms were restrained to be approximately isotropic. For compound $\mathbf{18{\bullet}H_2O{\bullet}}CH_2Cl_2$ the crystal under investigation was found to be again non-merohedrally twinned. The orientation matrices for the two components were identified using the program Cell Now,[6] and the two components were integrated using Apex2, resulting in a total of 43194 reflections. 731 reflections (376 unique) involved component 1 only (mean $I/\sigma = 33.0$), 720 reflections (374 unique) involved component 2 only (mean $I/\sigma = 28.2$), and 41743 reflections (17588 unique) involved both components (mean $I/\sigma = 5.1$). The exact twin matrix identified by the integration program was found to be -0.99923 0.00096 -0.00098, -0.00128 -1.00085 -0.00081, 0.14795 -0.00111 0.99182. The data were corrected for absorption using Twinabs,[7] and the structure was solved using direct methods with only the non-overlapping reflections of component 1. The structure was refined using the hklf 5 routine with all reflections of component 1 (including the overlapping ones) below a d-spacing threshold of 0.84 Å, resulting in a BASF value of 0.413(2). The Rint value given is for all reflections before the cutoff at d = 0.84 Å and is based on agreement between observed single and composite intensities and those calculated from refined unique intensities and twin fractions (Twinabs). One of the methylene chloride molecules is disordered over two positions with an occupancy rate for the major component of 0.65(2). The two disordered carbon atoms were constrained to have identical ADPs and C-Cl distances within the disordered sections were restrained to be the same within a standard deviation of 0.02 Å.

Synthesis of ($Tp^{tBu,Me}$)ZnEt

This compound was synthesized as previously reported.[8]

Synthesis of ($Tp^{tBu,Me}$)Zn(*p*-$OC_6H_4(NO_2)$)

In the literature,[9] this compound was synthesized by the use of ($Tp^{tBu,Me}$)ZnH and p-nitrophenol. We have synthesized this compound in the following manner: A solution of ($Tp^{tBu,Me}$)ZnEt (0.057 g, 0.110 mmol) in ~0.7 mL of C_6D_6 was combined with p-nitrophenol (0.016g, 0.115 mmol) in an NMR tube. The NMR tube was then sealed under an N_2 atmosphere and heated at 70˚C for 2 days. The progress of the reaction was monitored by ^{1}H-NMR spectra taken at different time intervals. After completion of the reaction, a light yellow product was isolated by removing the solvent under vacuum. This product was purified by recrystallization from toluene and hexane (1:1) and isolated in 74% yield (0.051 g). ^{1}HNMR in C_6D_6 and HR CI-MS data confirmed the formation of ($Tp^{tBu,Me}$)Zn(*p*-$OC_6H_4(NO_2)$).[9]

Elemental Analysis:

In order to achieve acceptable C, H, and N values we repeated analysis of some of the samples and the best data of those are reported as follow:

Found C 47.05, H 7.18, N 19.36, calcd. for ($Ttz^{tBu,Me}$)Zn(OCH_2CF_3) (**1**) C 46.76, H 6.65, N 21.34.

Found C 55.45, H 4.22, N 20.94, calcd. for ($Ttz^{Ph,Me}$)Zn(OCH_2CF_3) **(2).** C 53.52, H 4.18, N 19.37.

Found C 42.97, H 6.43, N 21.73, calcd. for ($Ttz^{tBu,Me}$)Zn($OCH(CF_3)_2$) **(3)** C 43.75, H 5.81, N 19.17.

Found C 49.39, H 4.05, N 16.12, calcd. for $(Ttz^{Ph,Me})Zn(OCH(CF_3)_2)$ (**4**) C 50.13, H 3.65, N 17.54).

Found C 55.40, H 7.35, N 19.09 calcd. for $(Ttz^{tBu,Me})Zn(OC_6H_5)$ (**5**) C 55.45, H 7.24, N 21.55.

Found C 60.46, H 4.87, N 18.75, calcd. For $(Ttz^{Ph,Me})Zn(OC_6H_5)$ **(6)** C 61.46, H 4.69, N 19.55.

Found C 51.22, H 6.18, N 20.08, calcd. for $(Ttz^{tBu,Me})Zn(p\text{-}OC_6H_4(NO_2))$ **(9)** C 51.48, H 6.56, N 22.24.

Found C 56.40, H 4.33, N 19.22, calcd. for $(Ttz^{Ph,Me})Zn(p\text{-}OC_6H_4(NO_2))$ $\mathbf{10_{cp}}$ C 57.45, H 4.24, N 20.30

Figure SI-1. a) Hydrogen bonds in the structure of $(Ttz^{Ph,Me})Zn(p\text{-}OC_6H_4(NO_2))\bullet H_2O$ (**10**$_{\mathbf{H2O}}$). b) Formation of a two-dimensional structure via H-bonds in this structure. [Color code: red-Oxygen, blue-Nitrogen, purple-Zinc, pink-Boron].

(a)

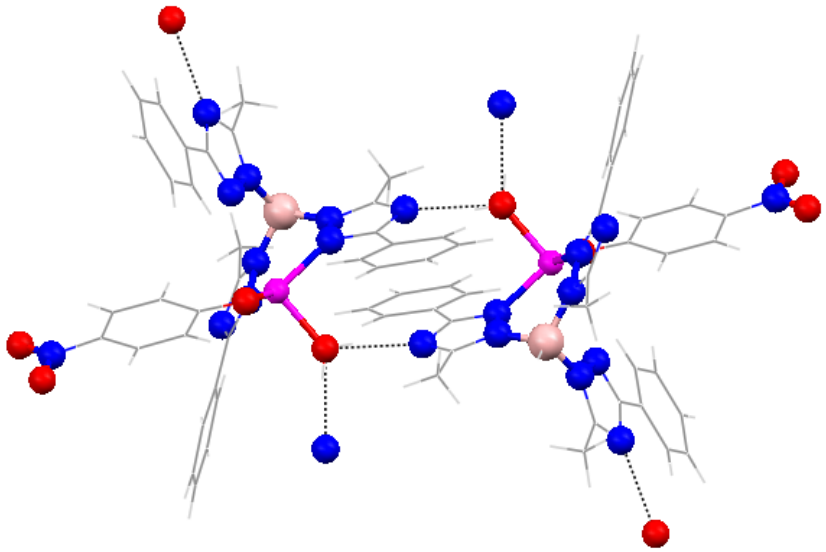

(b)

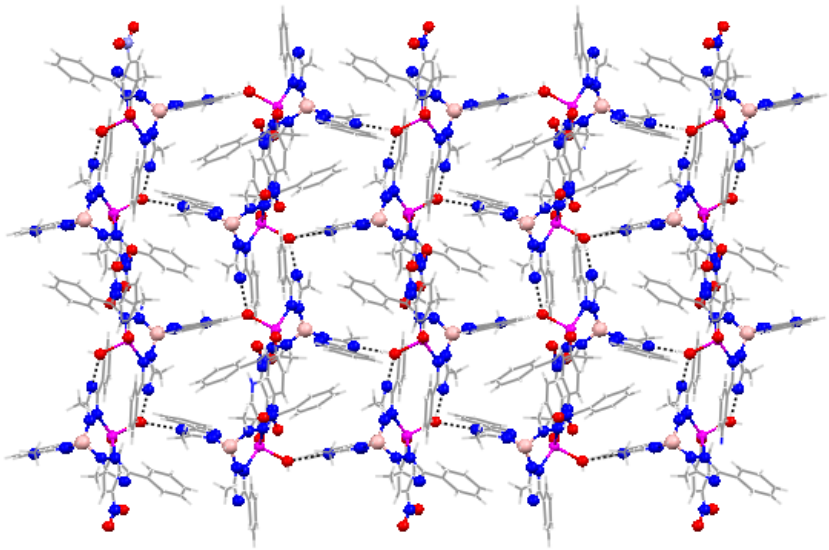

Preparation of stock solutions of Ttz$^{t\text{Bu,Me}}$ZnEt, Tp$^{t\text{Bu,Me}}$ZnEt and *p*-nitrophenol

A 10 mL volumetric flask was charged with Ttz$^{t\text{Bu,Me}}$ZnEt (0.015g, 0.02888 mmol, concentration = 2.888 mM) or Tp$^{t\text{Bu,Me}}$ZnEt (0.013g, 0.0252 mmol, concentration = 2.520 mM) and filled with dry toluene. The contents were mixed thoroughly and the resultant clear solutions were used as the stock solutions for kinetic experiments. These solutions were further diluted with toluene to acquire the desired molarity of the solution for various experiments.

A solution of *p*-nitrophenol in toluene was prepared in a 25 mL volumetric flask from *p*-nitrophenol (0.008g, 0.0575 mmol, concentration = 2.30 mM). 1.0 mL of this solution was transferred to another 25 mL of volumetric flask and then the flask was filled with toluene and the contents were mixed thoroughly. The final concentration of this solution was calculated as 0.092 mM and this solution was used for all the kinetic measurements.

UV/Vis spectra and Beer-Lambert Law plots for (Ttz^{tBu,Me})Zn(*p*-OC$_6$H$_4$(NO$_2$)) and (Tp^{tBu,Me})Zn(*p*-OC$_6$H$_4$(NO$_2$))

Figure SI-2. (a) UV/Vis spectra of (Ttz^{tBu,Me})Zn(*p*-OC$_6$H$_4$(NO$_2$)) in toluene at room temperature in varying concentration (λ_{max} = 337 nm). **Color code - Conc. (M) / absorbance:** Blue - 0.000038 / 0.522071, Red - 0.000031 / 0.422603, Green - 0.0000228 / 0.321169, Black - 0.0000153 / 0.236365, Orange - 0.0000097 / 0.164741; **(b)** Beer-Lambert Law plot.

(a)

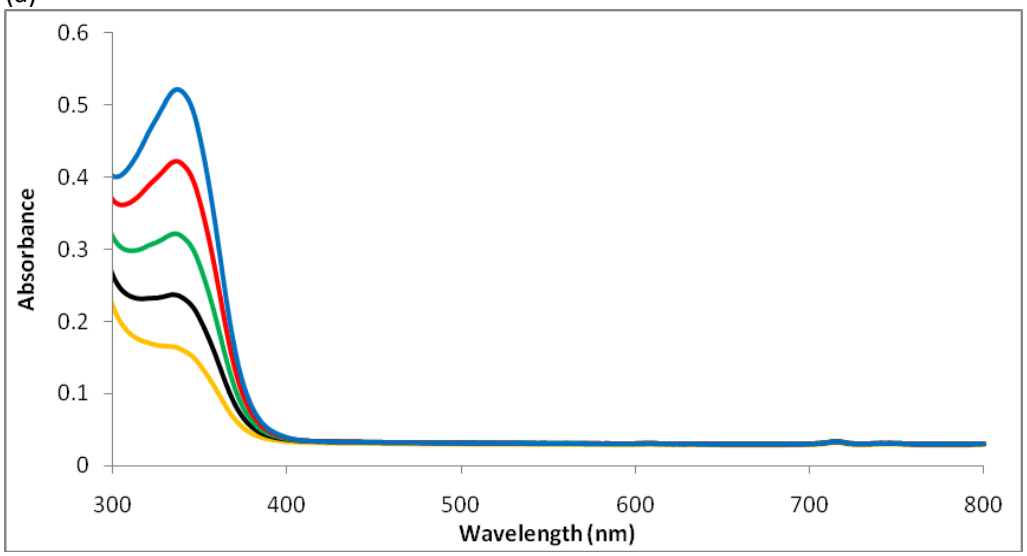

(b)

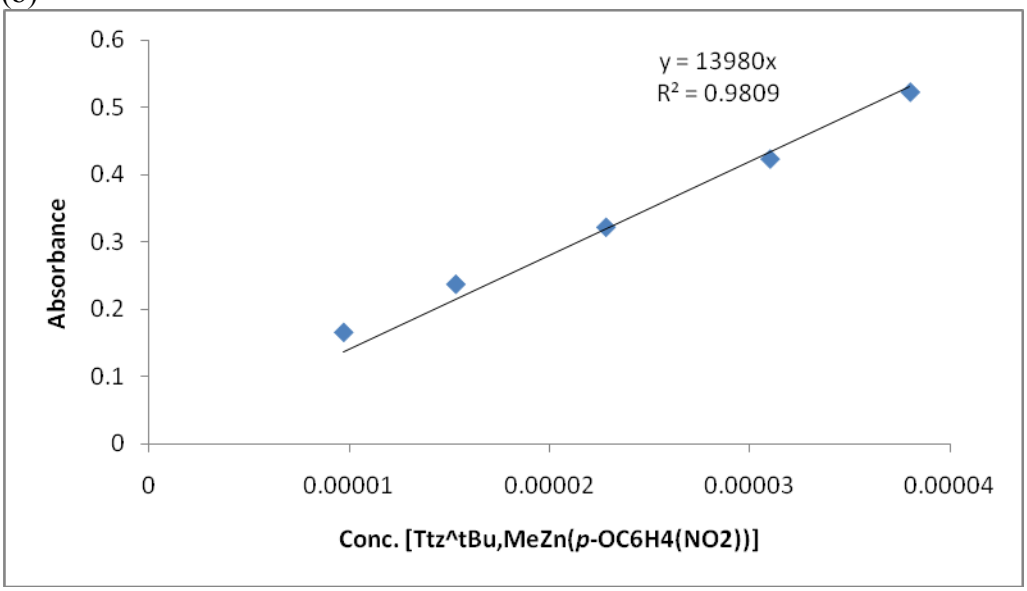

Figure SI-3. (a) UV/Vis spectra of ($Tp^{tBu,Me}$)Zn(*p*-$OC_6H_4(NO_2)$) in toluene at room temperature in varying concentration (λ_{max} = 347 nm). **Color code – Conc. (M) / absorbance**: Blue – 0.0001636 / 2.322302, Red - 0.00006544 / 0.953959, Green - 0.00004902 / 0.732343, Black - 0.00003268 / 0.506736, Orange - 0.00001634 / 0.289403; **(b)** Beer-Lambert Law plot.

(a)

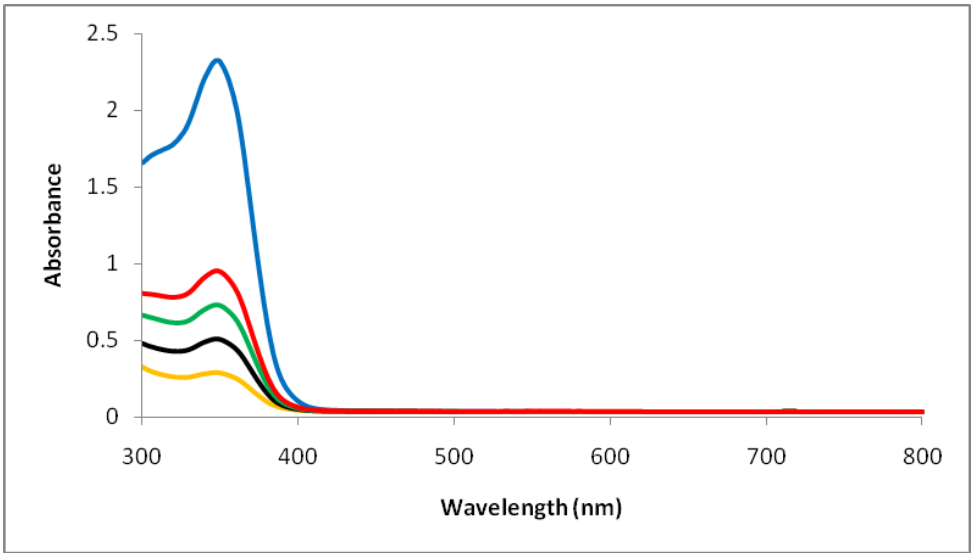

(b)

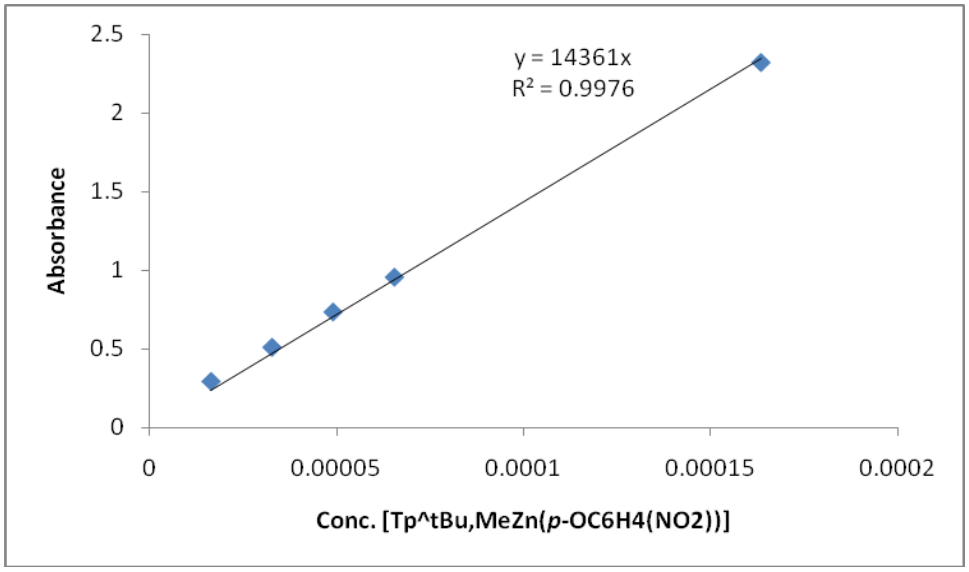

Representative example of kinetic analysis procedure.

In the present report, kinetic studies were all performed for the conversion of LZnEt (L = $Ttz^{tBu,Me}$, $Tp^{tBu,Me}$) to LZn(*p*-$OC_6H_4(NO_2)$) in the presence of p-nitrophenol. The concentration of p-nitrophenol kept constant for all the kinetic experiments and only variation in the concentration of LZnEt was made. These reactions were assumed to be of pseudo first order. In a typical experiment, a solution of p-nitrophenol (1.5 mL) and LZnEt (1.5 mL) in toluene with known concentration was mixed in a special designed air free UV cell. The experiments were done at 95ºC and the data points were taken at 15 minute intervals. After desired reaction time, absorbance data points along with molar absorption coefficients were used to calculate the concentration of p-nitrophenol (**A**) consumed and LZn(*p*-$OC_6H_4(NO_2)$) (**B**) formed. Equations 1 and 2 were used to calculate the concentration of **A** and **B**, but equation 2 was found to give a more accurate concentration of **B**. This is due to the fact that the extinction coefficients do not differ very much for reactant A and product B at 296nm; thus the absorbance at 337nm shows a much greater change during the reaction. The concentration of **B** at each time is equal to the initial concentration of A minus the concentration of A at that time: $[B]_t = [A]_0 - [A]_t$. Thus we used equation (2) to calculate the concentration of A at any given time by substituting for $[B]_t$ and solving for $[A]_t$, giving equation 3.

$$A_{296} = \varepsilon_{296}{}^{A} \times [A]_t + \varepsilon_{296}{}^{B} \times [B]_t \qquad (1)$$

$$A_{337} = \varepsilon_{337}{}^{A} \times [A]_t + \varepsilon_{337}{}^{B} \times [B]_t \qquad (2)$$

$$[A]_t = [A_{337} - (\varepsilon_{337}{}^{B} \times [A]_0)] / [\varepsilon_{337}{}^{A} - \varepsilon_{337}{}^{B}] \qquad (3)$$

Fig SI-4. UV/Vis spectra (absorbance *vs.* wavelength) monitoring for the reaction between 1.5 mL of Ttz$^{t\text{Bu,Me}}$ZnEt (2.888 mM) and 1.5 mL of *p*-nitrophenol (0.092 mM) in toluene at 95°C.

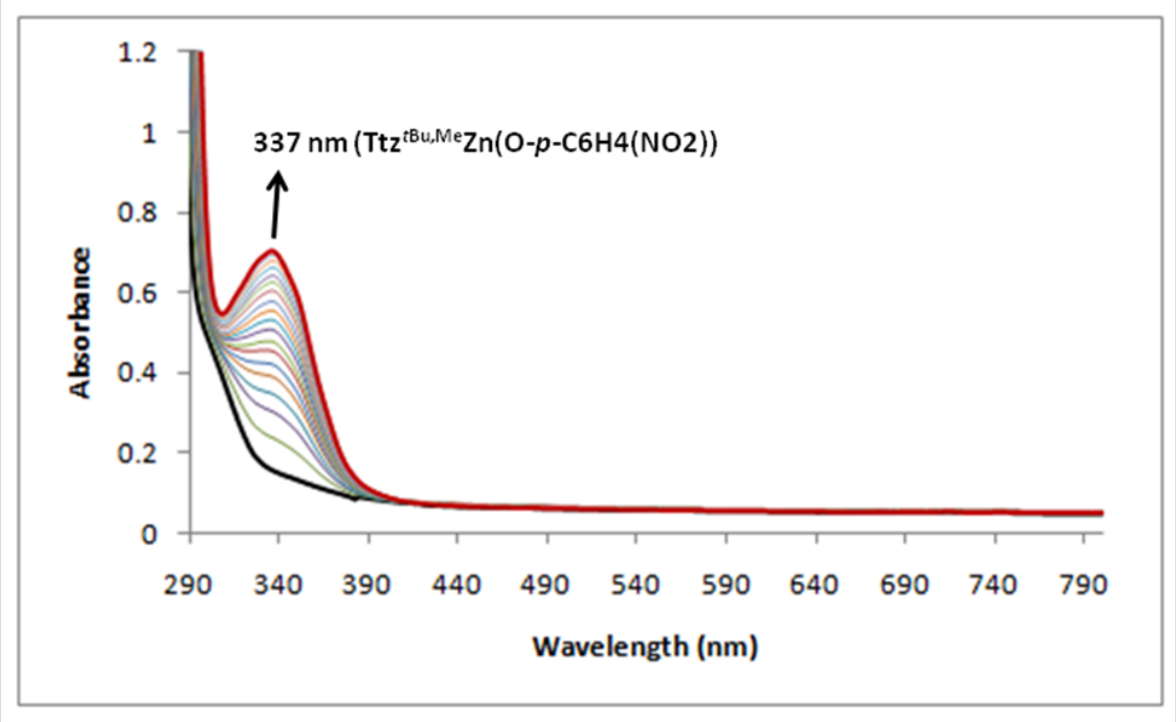

Figure SI-5. Plot of [p-nitrophenol] *vs.* time for 0.000578 M of Ttz$^{t\text{Bu,Me}}$ZnEt.

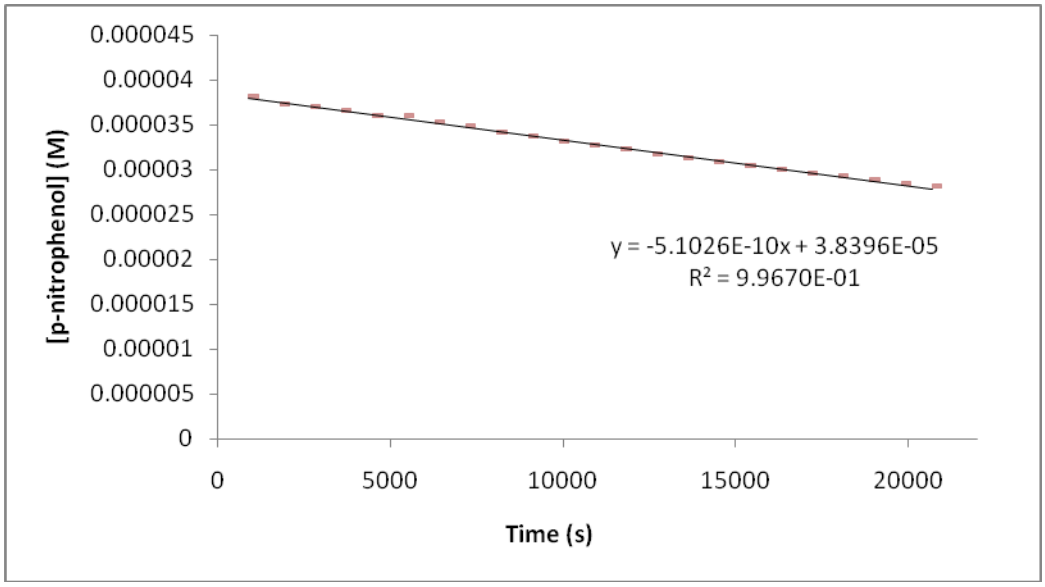

Figure SI-6. Plot of [p-nitrophenol] *vs.* time for 0.000693 M of Ttz$^{t\text{Bu,Me}}$ZnEt.

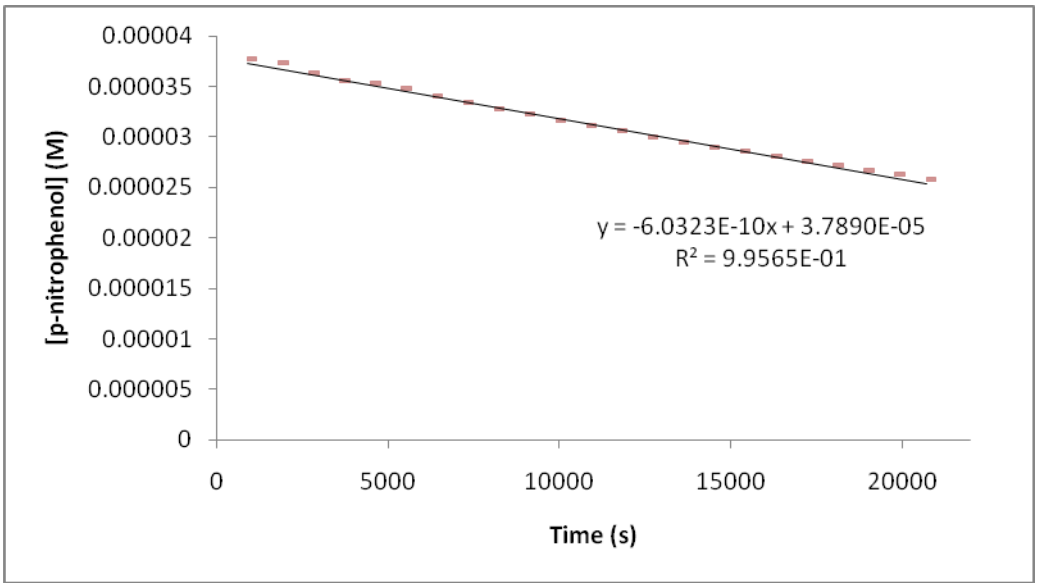

Figure SI-7. Plot of [p-nitrophenol] *vs.* time for 0.000866 M of Ttz$^{t\text{Bu,Me}}$ZnEt.

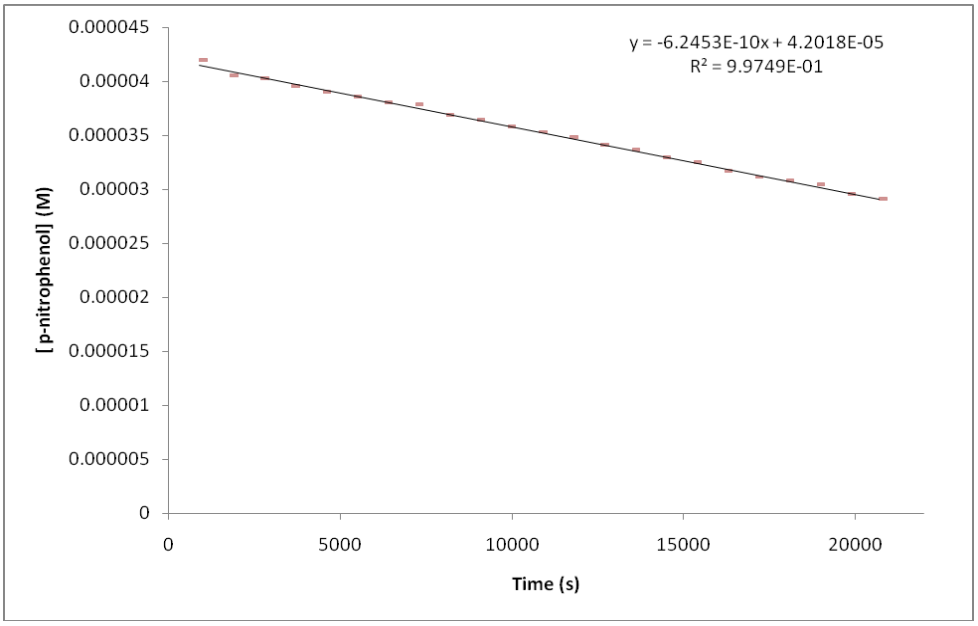

Figure SI-8. Plot of [p-nitrophenol] *vs.* time for 0.001018 M of Ttz$^{t\text{Bu,Me}}$ZnEt.

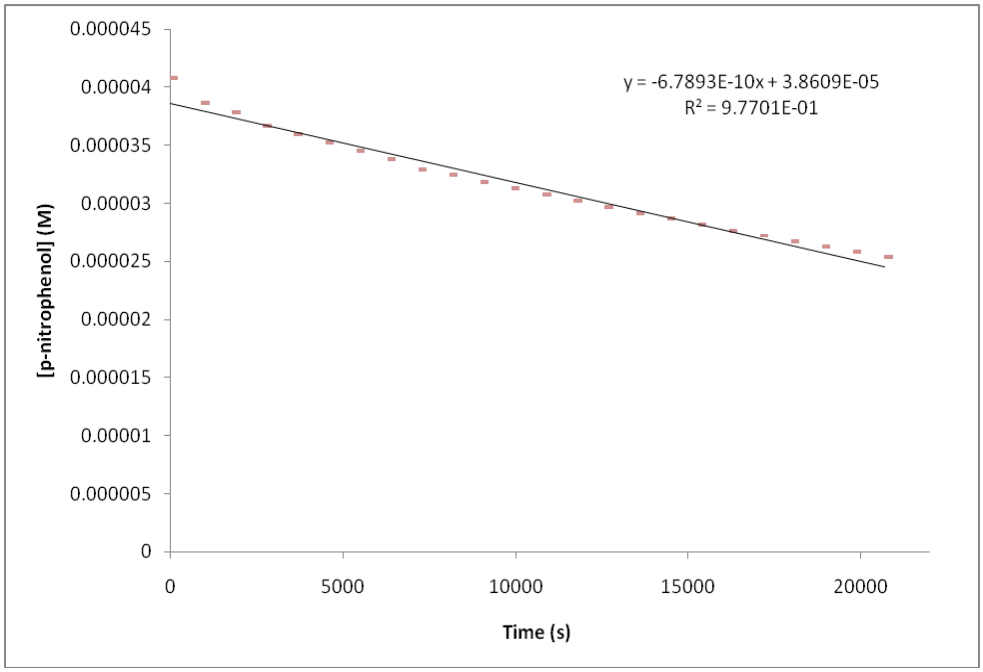

Figure SI-9. Plot of [p-nitrophenol] *vs.* time for 0.001155 M of Ttz$^{t\text{Bu,Me}}$ZnEt.

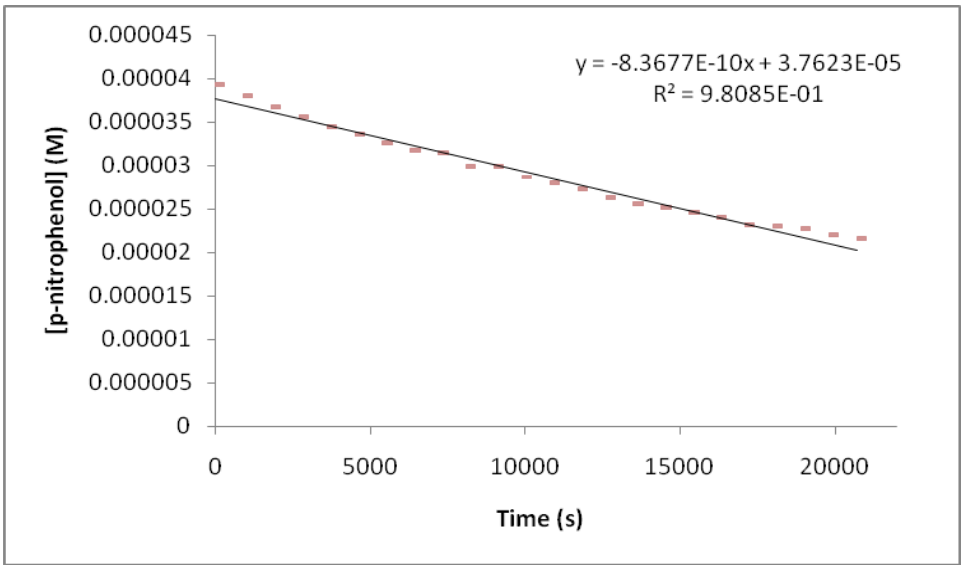

Figure SI-10. Plot of [p-nitrophenol] *vs.* time for 0.001444 M of Ttz$^{t\text{Bu,Me}}$ZnEt.

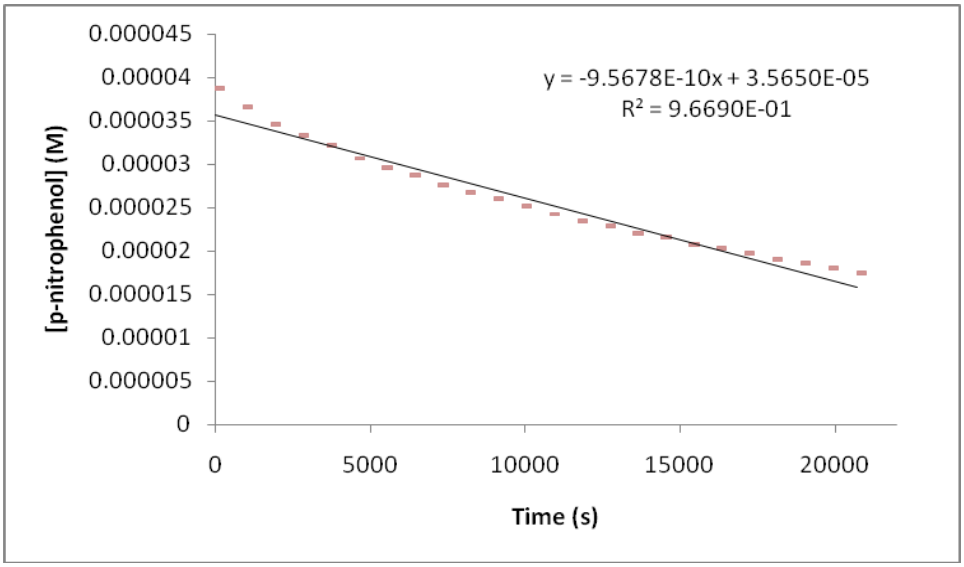

Fig SI-11. UV/Vis spectra (absorbance *vs.* wavelength) monitoring for the reaction between 1.5 mL of Tp$^{t\text{Bu,Me}}$ZnEt (2.520 mM) and 1.5 mL of *p*-nitrophenol (0.092 mM) in toluene at 95°C (First 23 cycles) (Blue line shows the spectrum of *p*-nitrophenol taken before mixing).

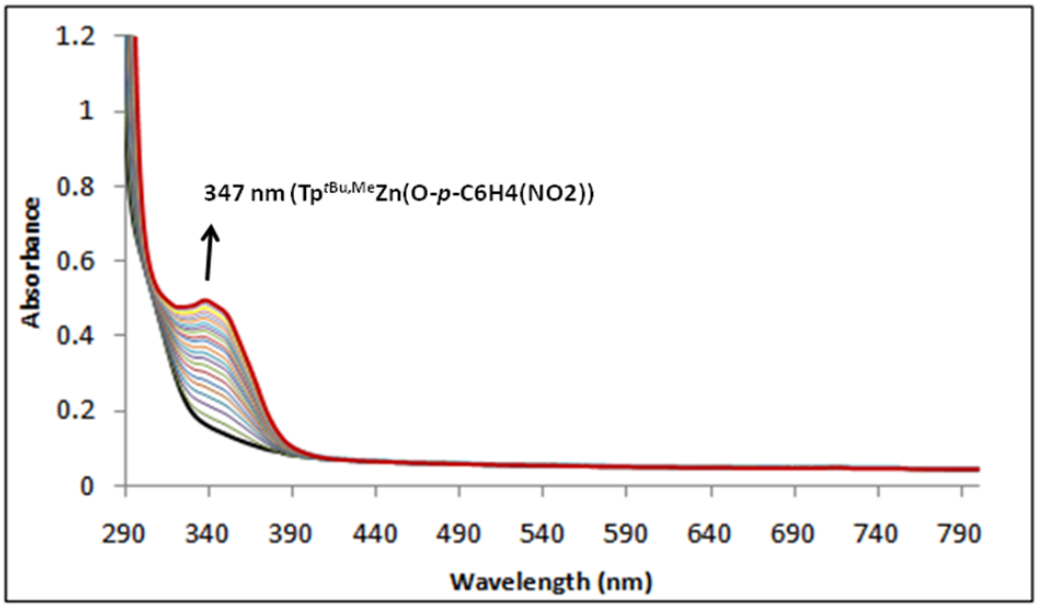

Figure SI-12. Plot of [p-nitrophenol] *vs.* time for 0.000527 M of Tp^{tBu,Me}ZnEt.

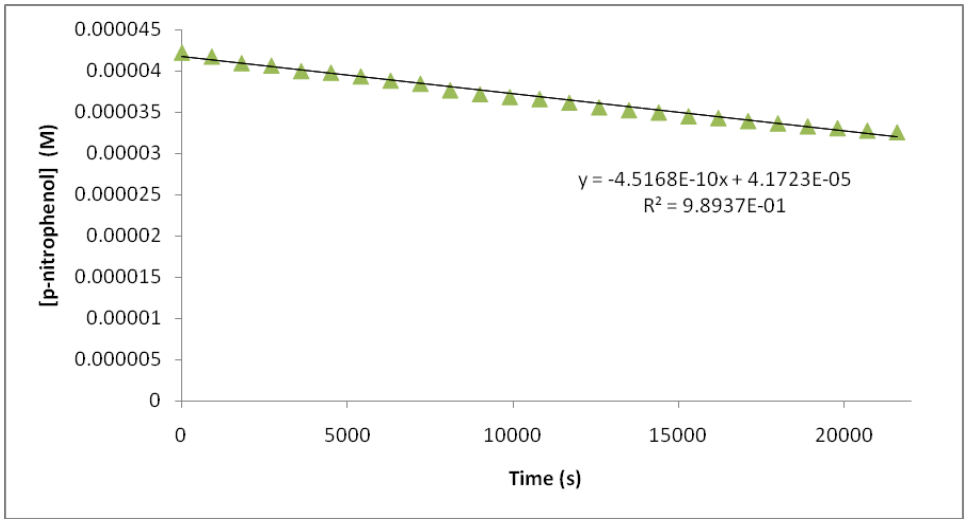

Figure SI-13. Plot of [p-nitrophenol] *vs.* time for 0.000702 M of Tp^{tBu,Me}ZnEt,

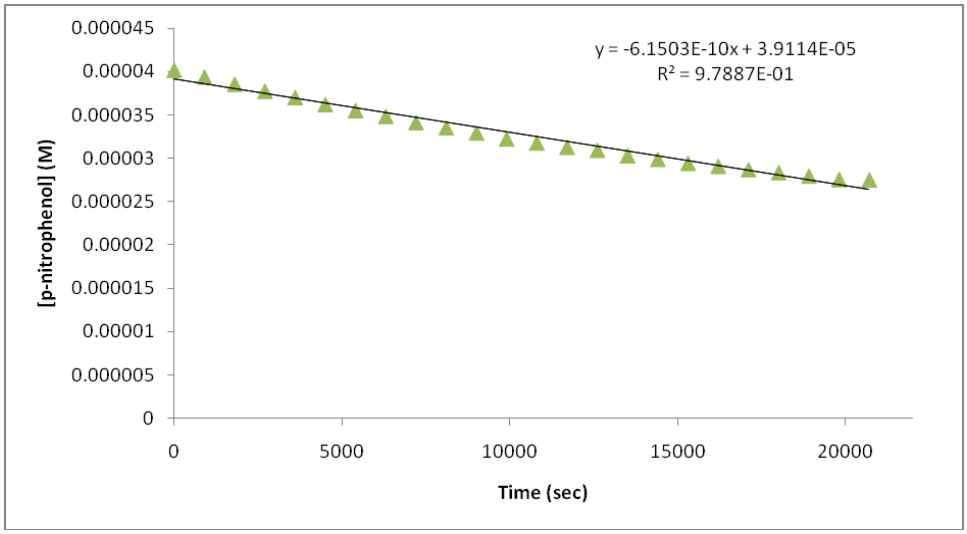

Figure SI-14. Plot of [p-nitrophenol] *vs.* time for 0.000878 M of Tp^{tBu,Me}ZnEt.

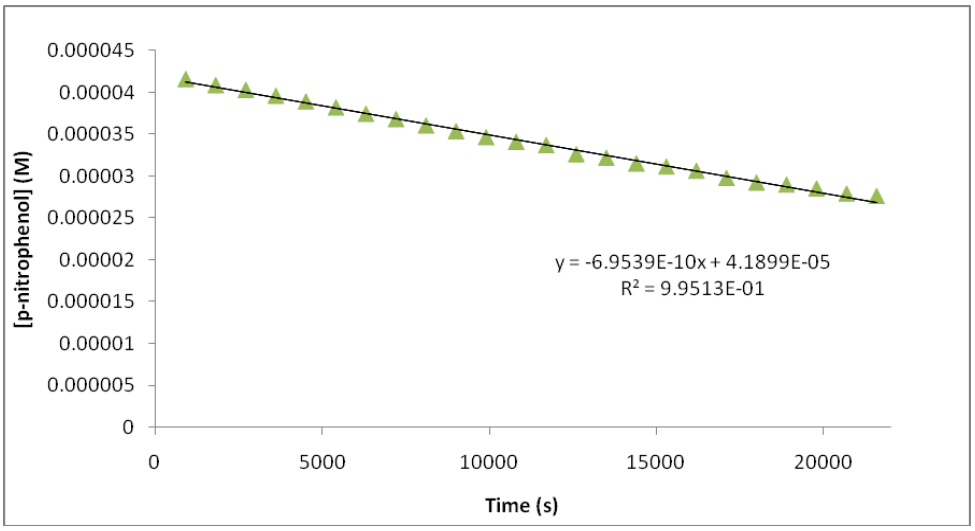

Figure SI-15. Plot of [p-nitrophenol] *vs.* time for 0.001008 M of Tp^{tBu,Me}ZnEt.

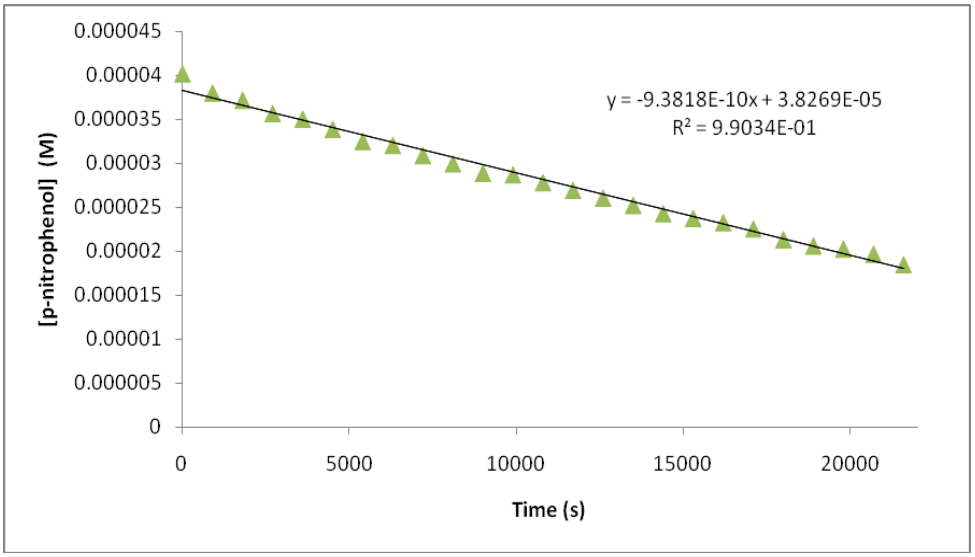

Figure SI-16. Plot of [p-nitrophenol] *vs.* time for 0.00126 M of $Tp^{tBu,Me}ZnEt$.

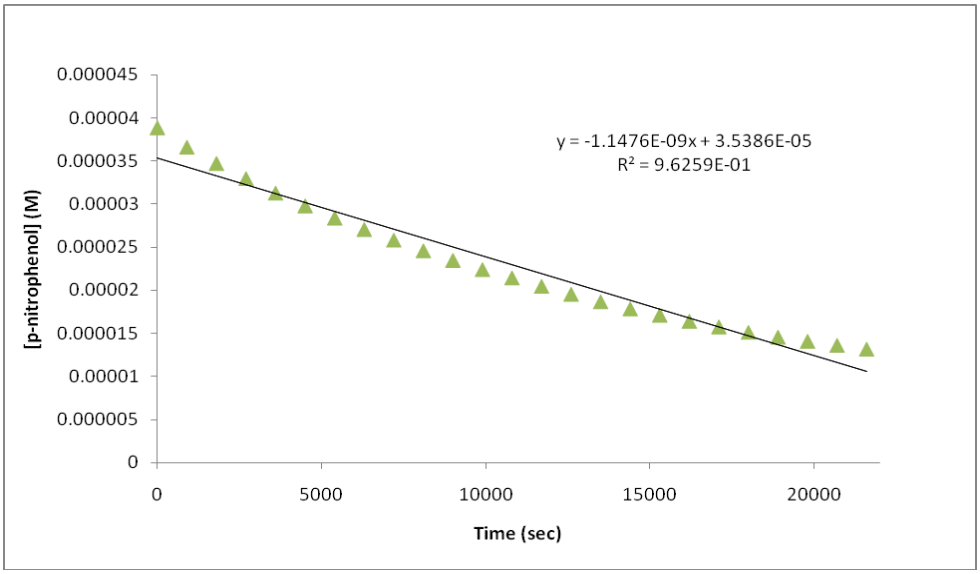

Figure SI-17. CI-MS spectrum of ($Ttz^{tBu,Me}$)Zn(OCH_2CF_3) (**1**).

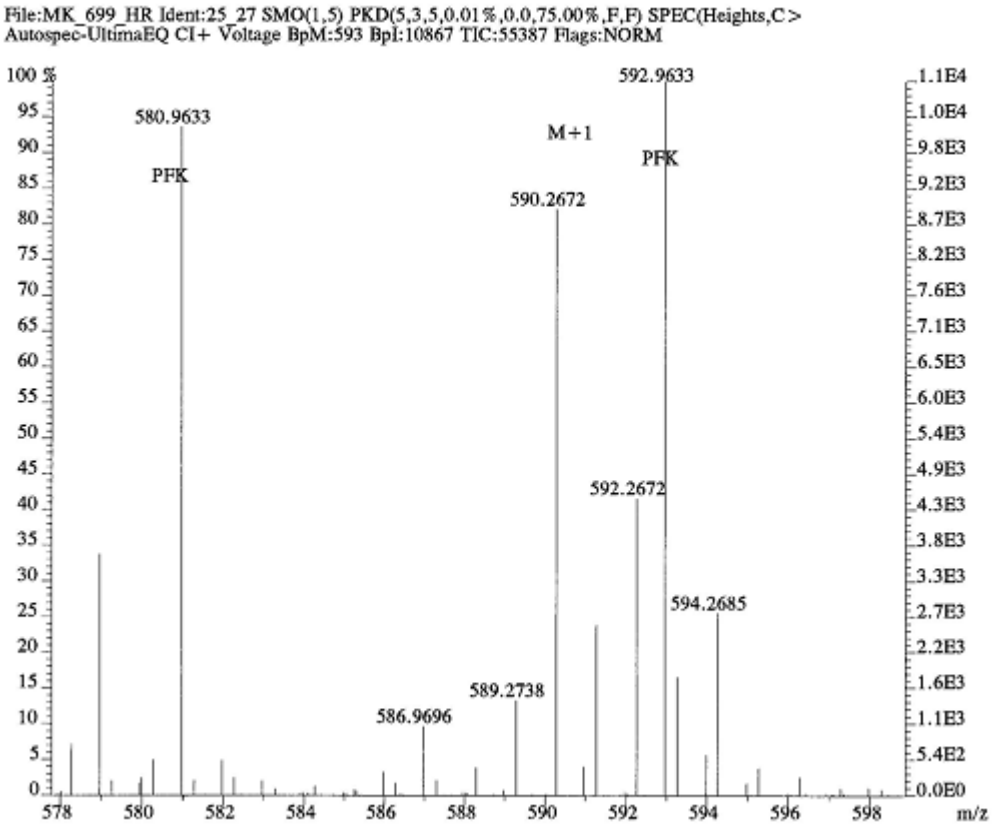

Calculated isotopic pattern for M+1

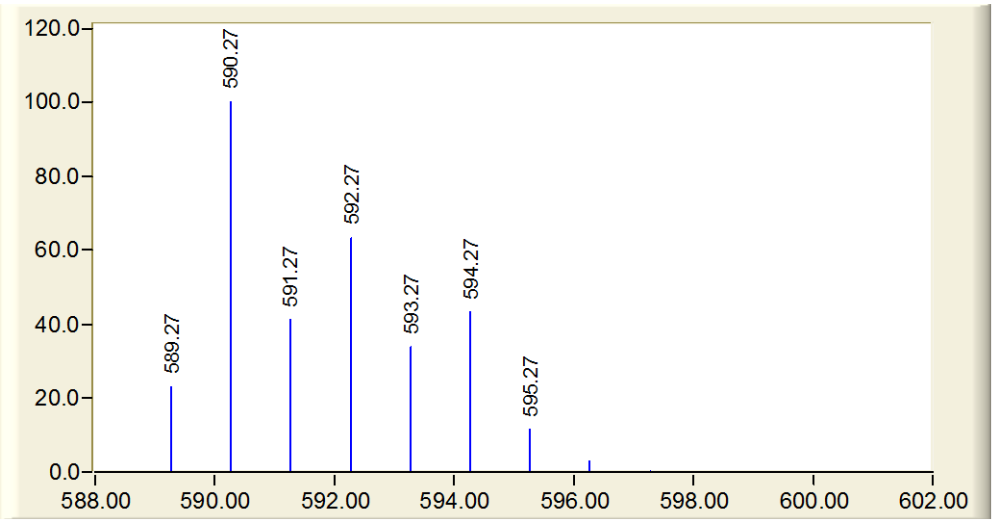

Figure SI-18. CI-MS spectrum of ($Ttz^{Ph,Me}$)Zn(OCH_2CF_3) (**2**).

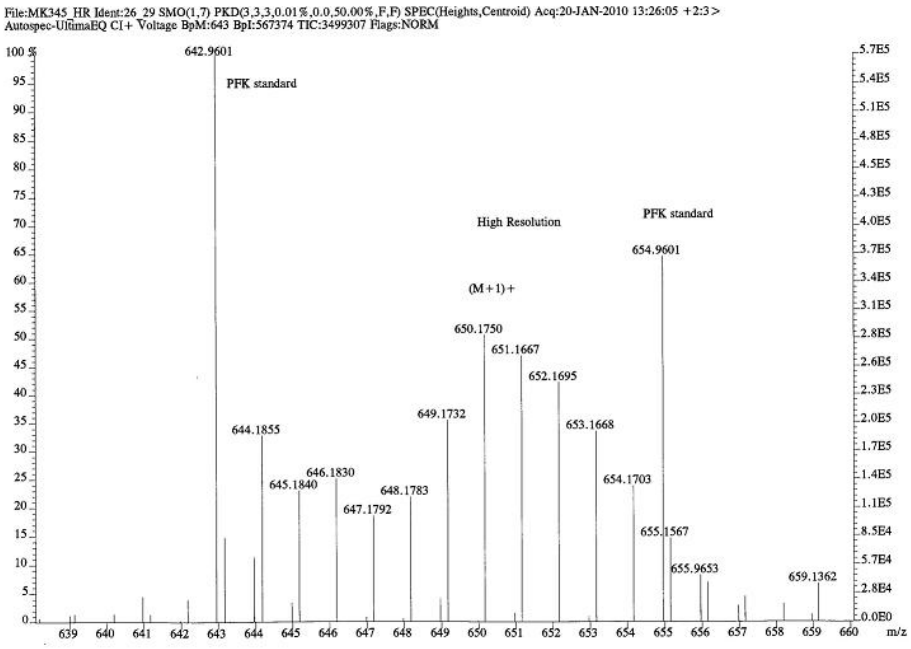

Calculated isotopic pattern for M+1

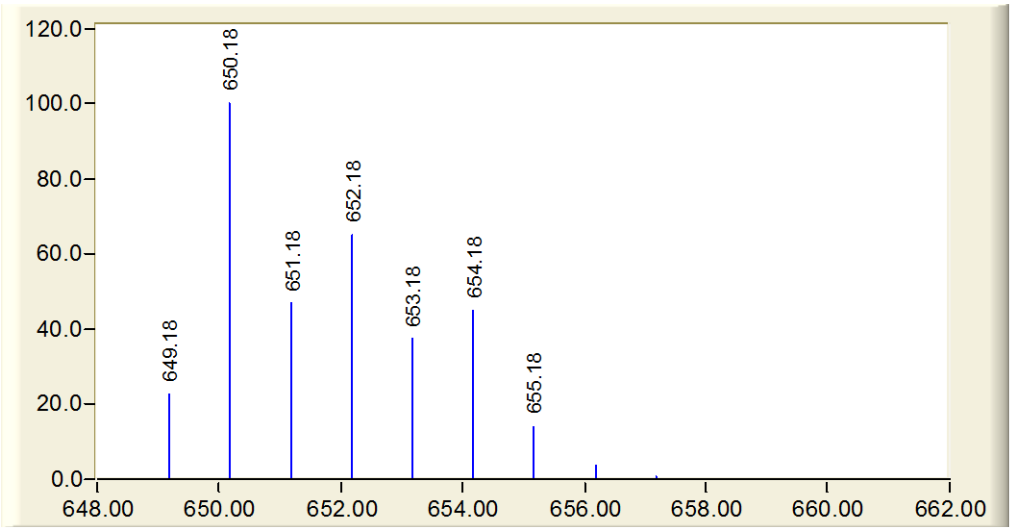

Figure SI-19. CI-MS spectrum of $(Ttz^{tBu,Me})Zn(OCH(CF_3)_2)$ (**3**).

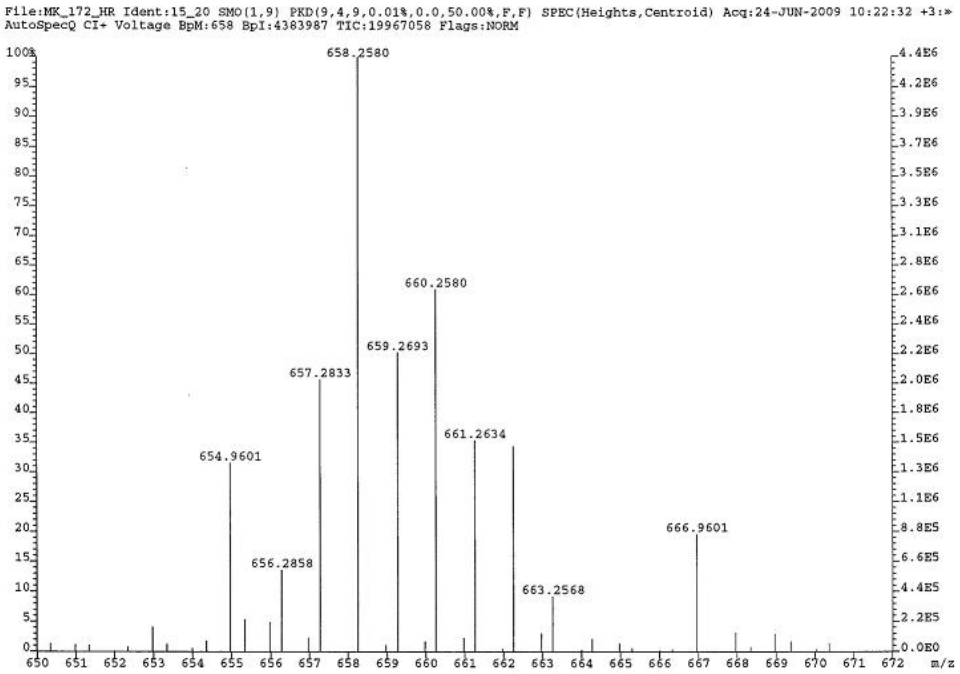

Calculated isotopic pattern for M+1

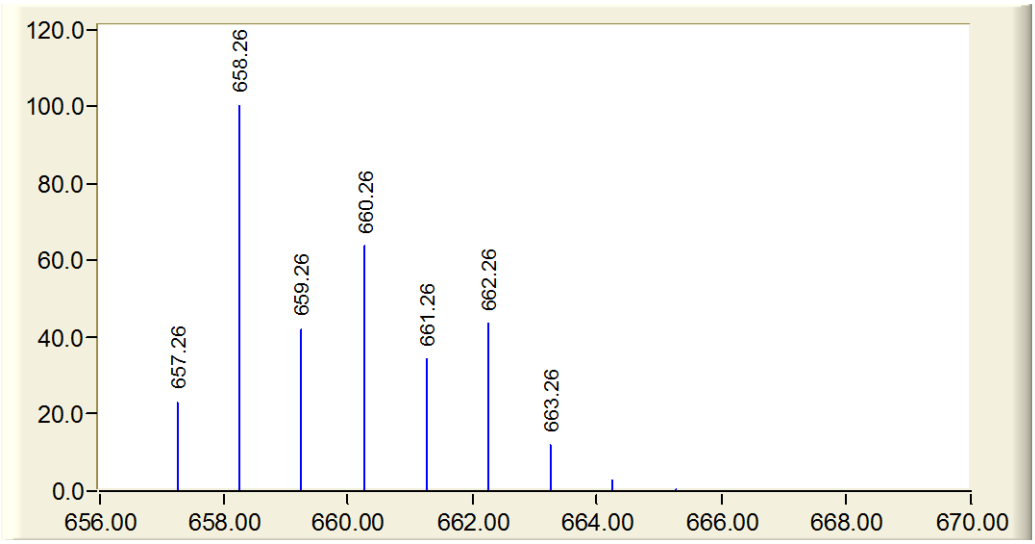

Figure SI-20. CI-MS spectrum of $(Ttz^{Ph,Me})Zn(OCH(CF_3)_2)$ (**4**).

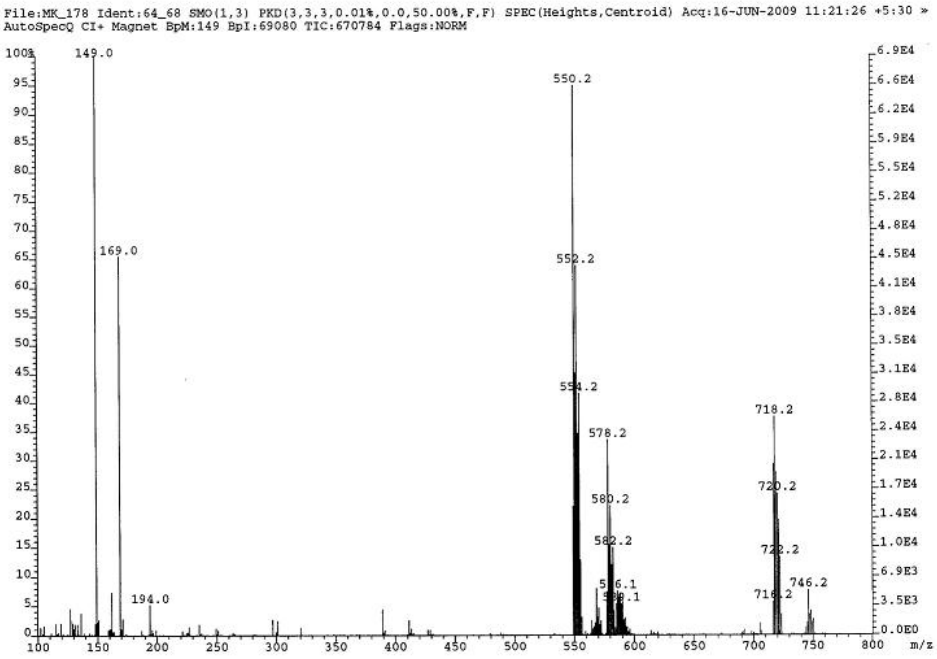

Calculated isotopic pattern for M+1

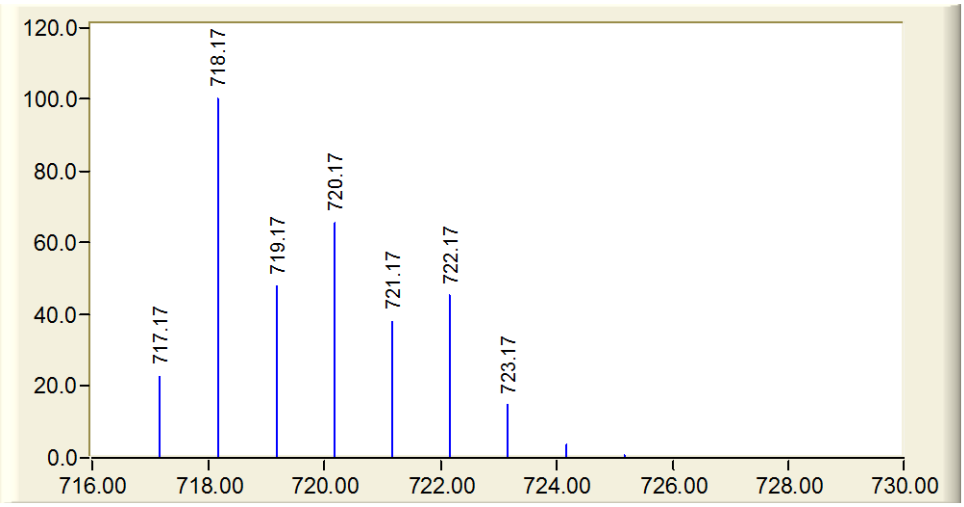

Figure SI-21. FAB-MS spectrum of (Ttz$^{t\mathrm{Bu,Me}}$)Zn(OPh) (**5**).

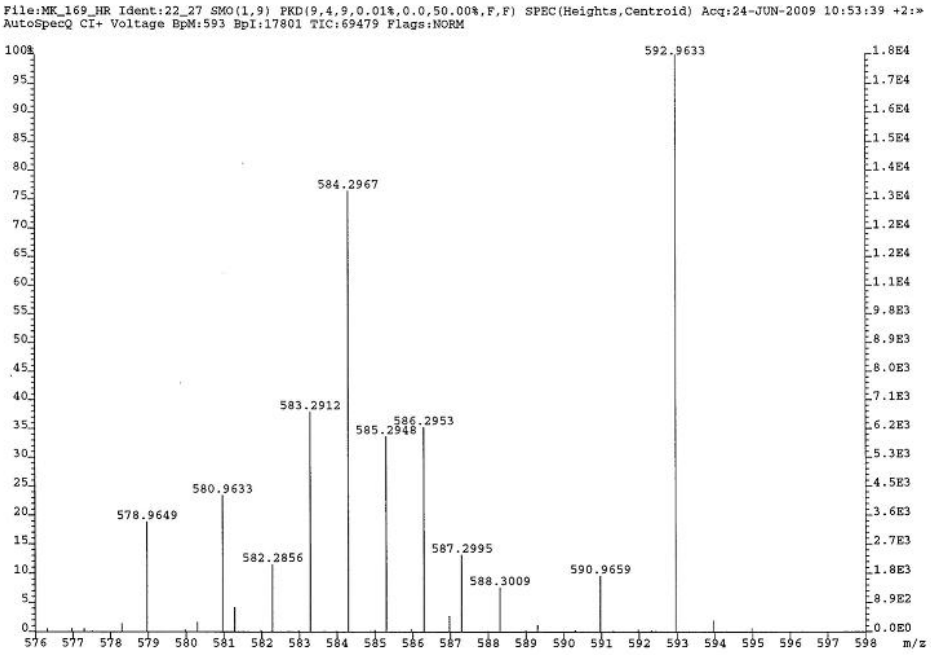

Calculated isotopic pattern for M+1

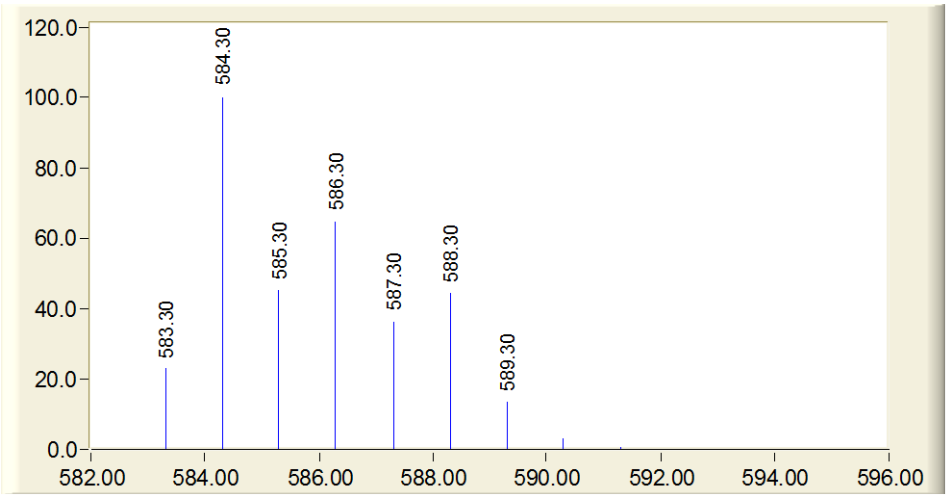

Figure SI-22. CI-MS spectrum of ($Ttz^{Ph,Me}$)Zn(OPh) (**6**).

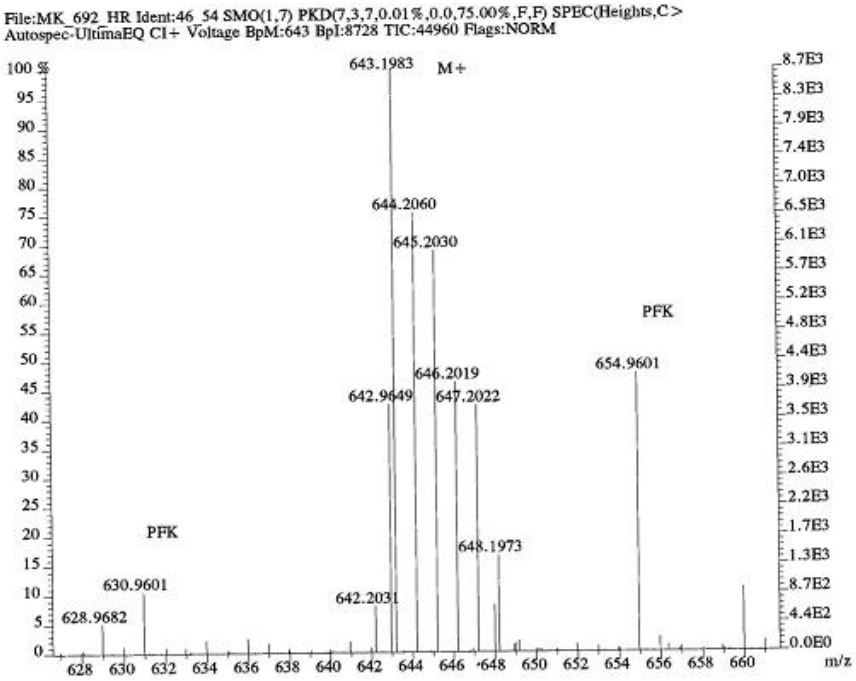

Calculated isotopic pattern for M+

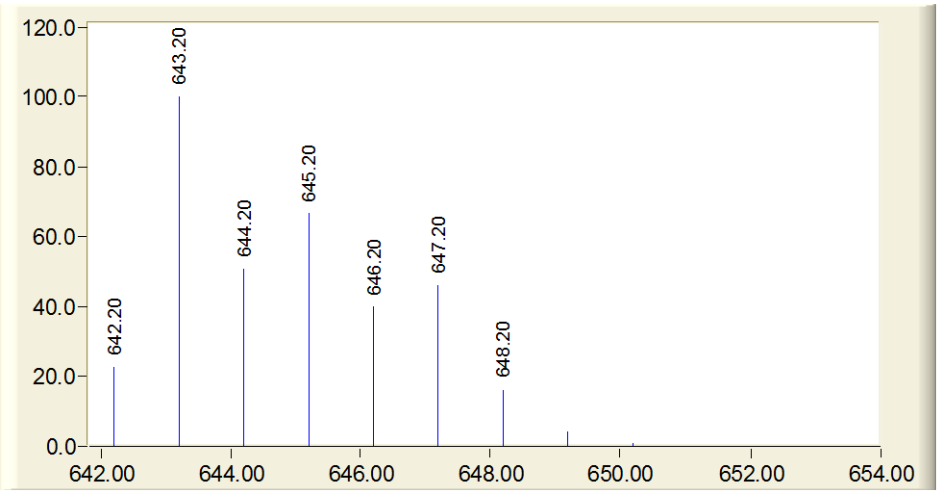

Figure SI-23. CI-MS spectrum of (Ttz$^{t\mathrm{Bu,Me}}$*)Zn(SPh) (**7**).

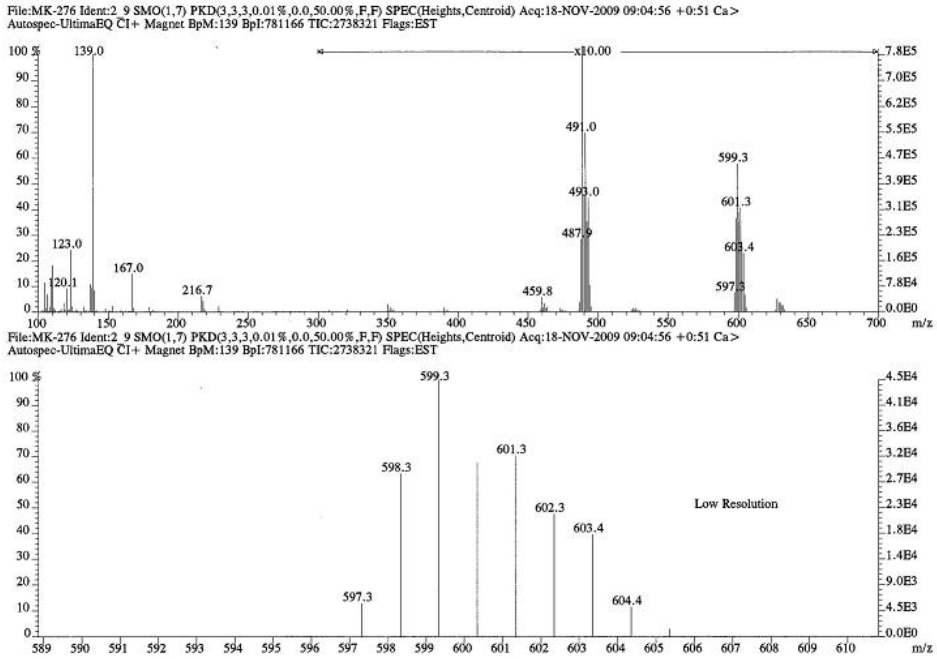

Calculated isotopic pattern for M+1

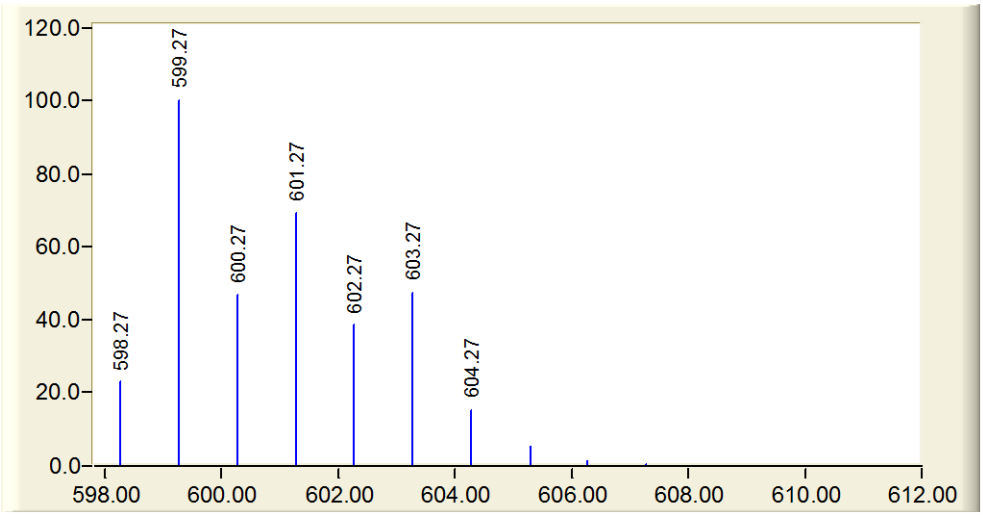

Figure SI-24. CI-MS spectrum of ($Ttz^{Ph,Me}$)Zn(SPh) (**8**).

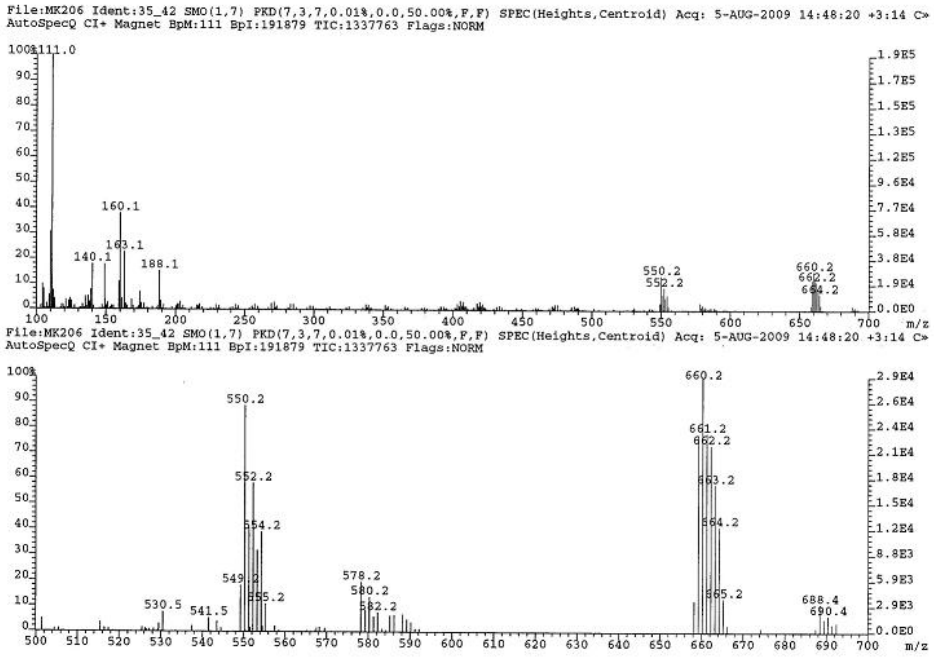

Calculated isotopic pattern for M+1

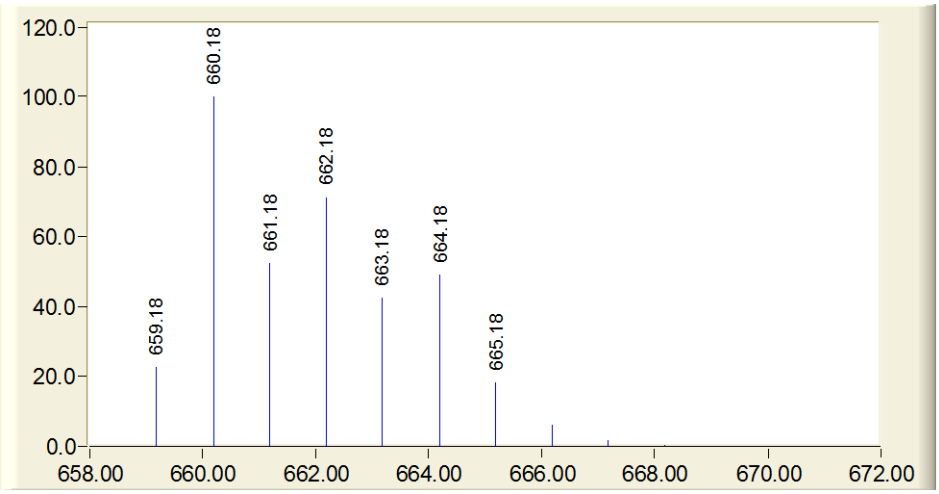

Figure SI-25. CI-MS spectrum of (Ttz$^{t\mathrm{Bu,Me}}$)Zn(*p*-OC$_6$H$_4$(NO$_2$)) (**9**).

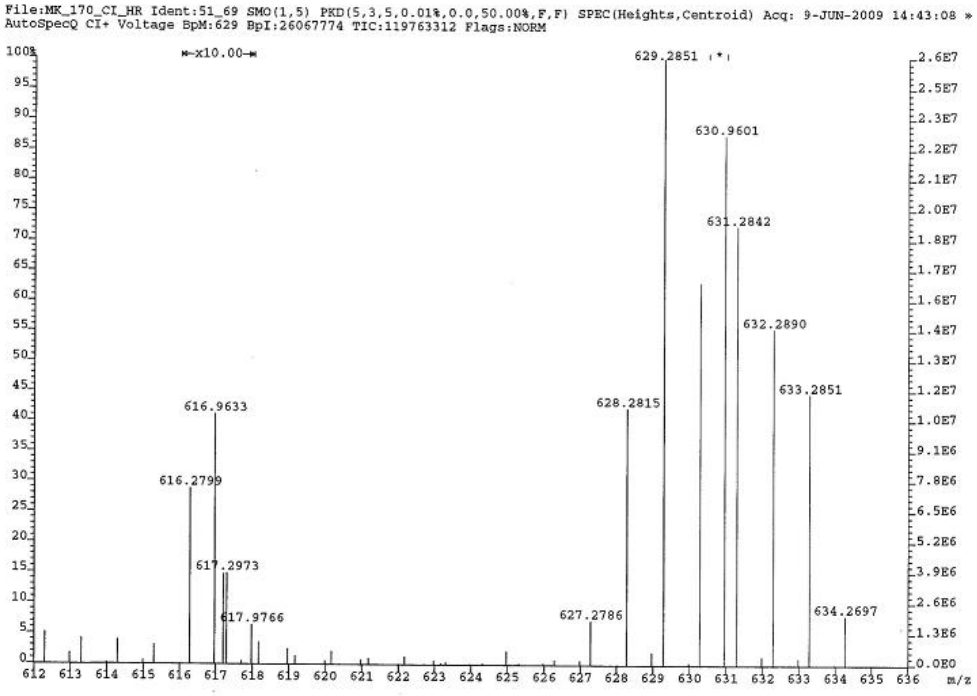

Calculated isotopic pattern for M+1

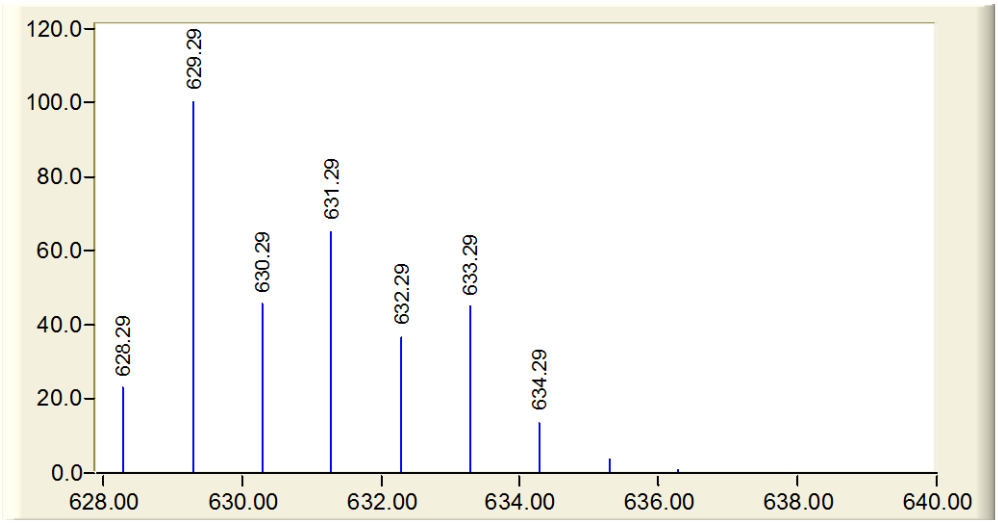

Figure SI-26. CI-MS spectrum of $(Ttz^{Ph,Me})Zn(p\text{-}OC_6H_4(NO_2))$ (**10**$_{\mathbf{CP}}$).

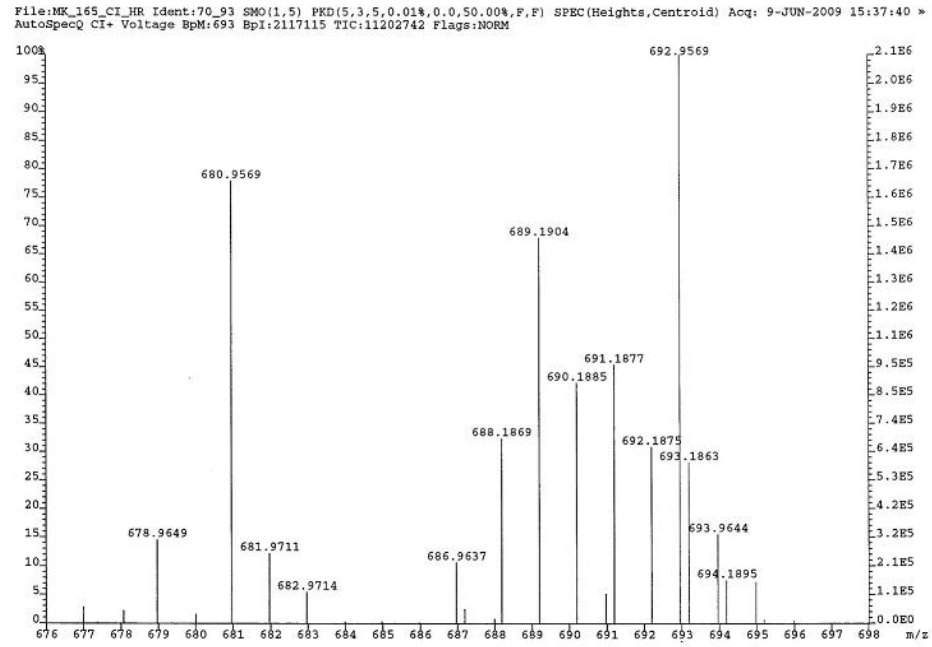

Calculated isotopic pattern for M+1

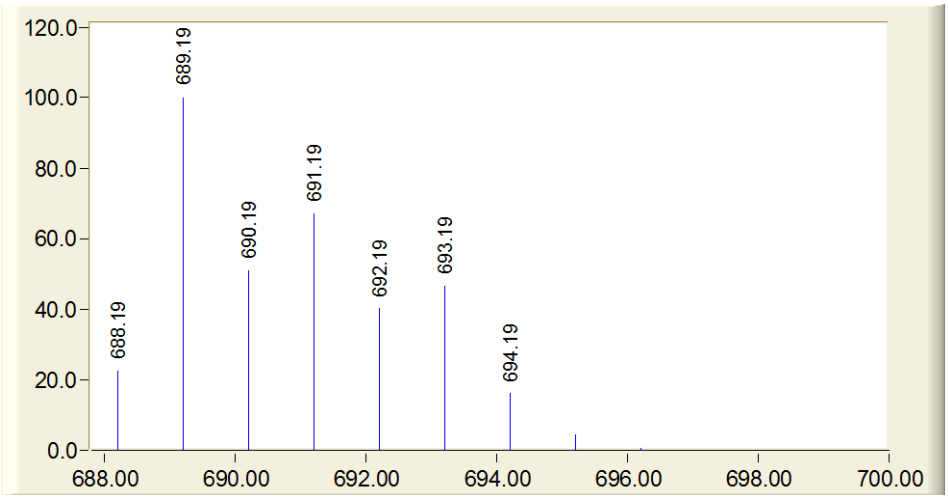

Figure SI-27. CI-MS spectrum of (Ttz$^{t\mathrm{Bu,Me}}$)Zn(acac) (**11**).

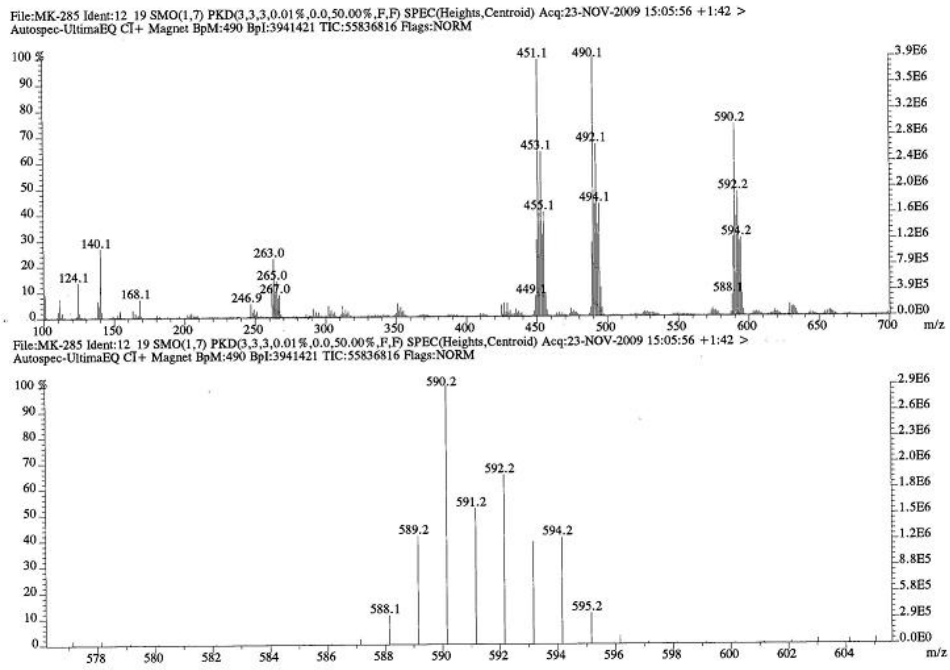

Calculated isotopic pattern for M+1

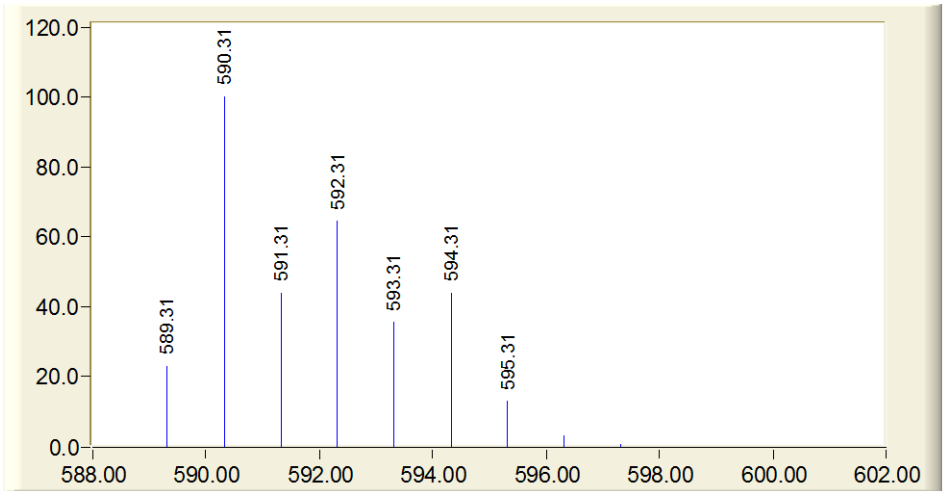

Figure SI-28. CI-MS spectrum of ($Ttz^{Ph,Me}$)Zn(acac) (**12**).

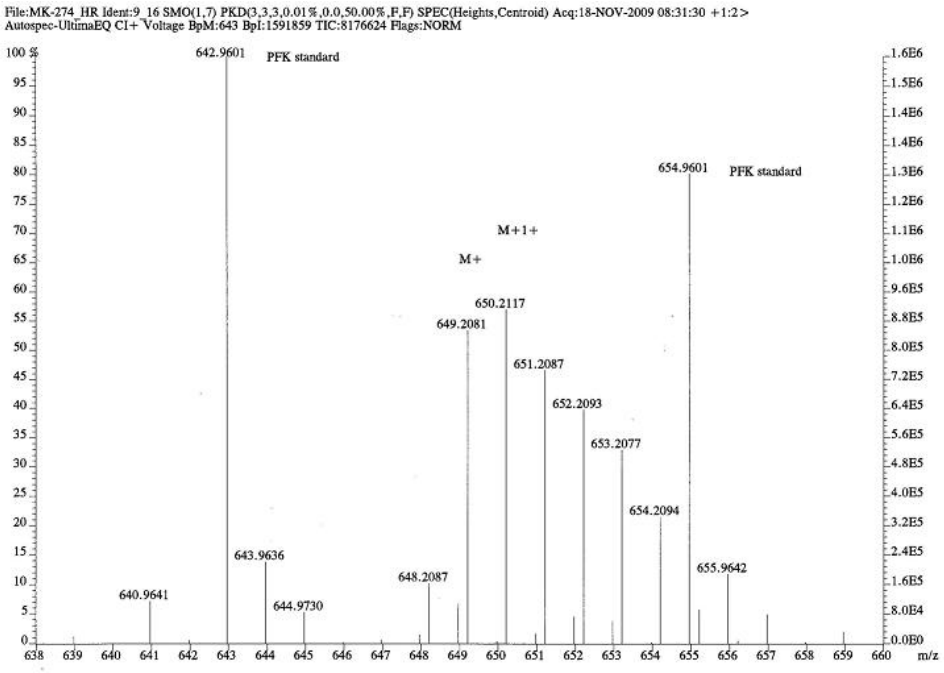

Calculated isotopic pattern for M+1

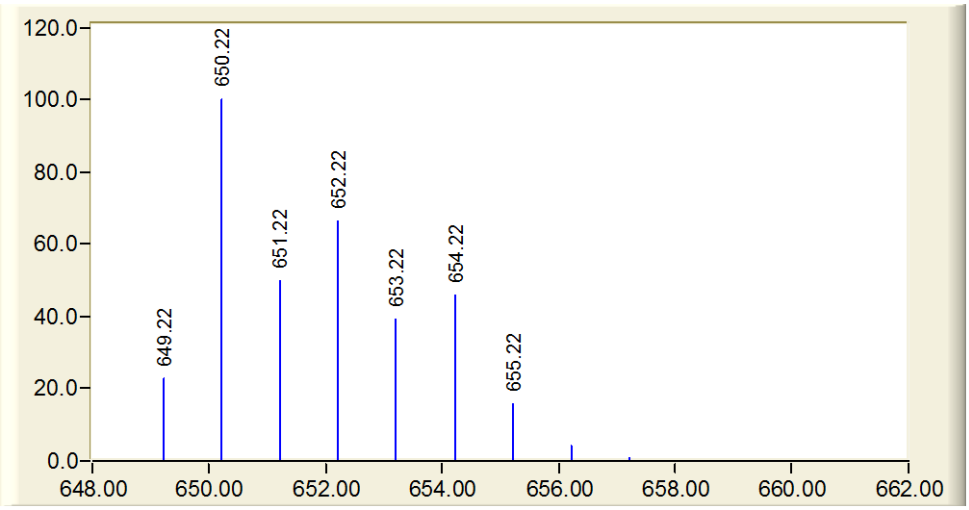

Figure SI-29. CI-MS spectrum of ($Ttz^{tBu,Me}$)Zn(O_3SCF_3) (**16**).

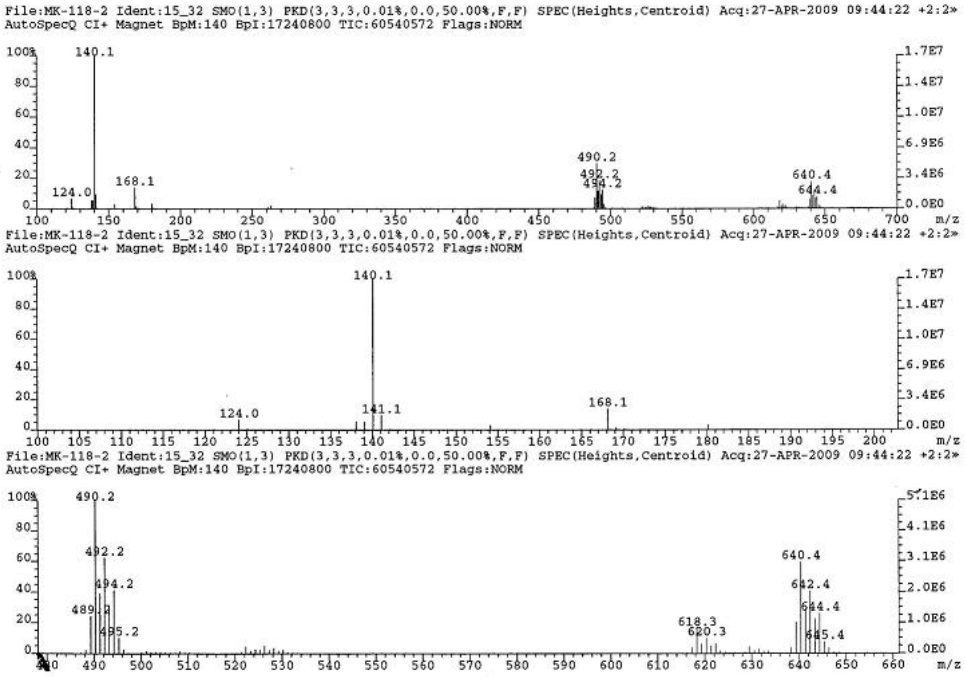

Calculated isotopic pattern for M+1

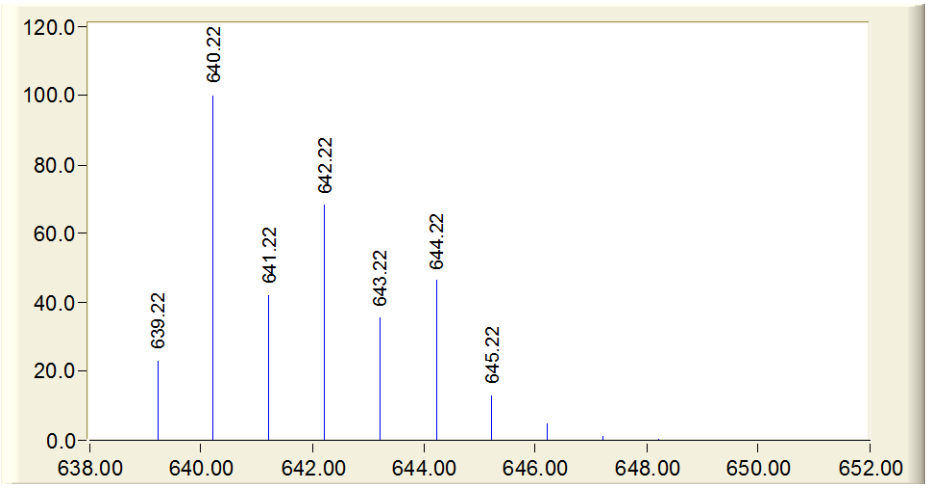

Figure SI-30. FAB-MS spectrum of $Htz^{tBu,Me}$.

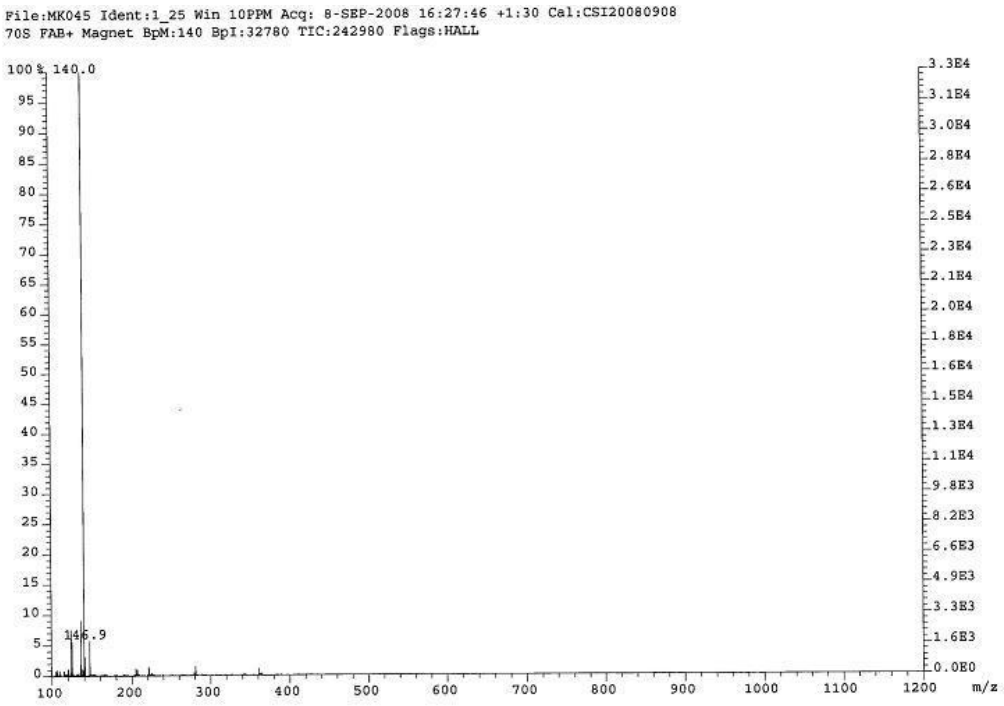

Figure SI-31. ^1H NMR (C_6D_6) spectrum of $Ttz^{tBu,Me}ZnOCH_2CF_3$ (**1**)

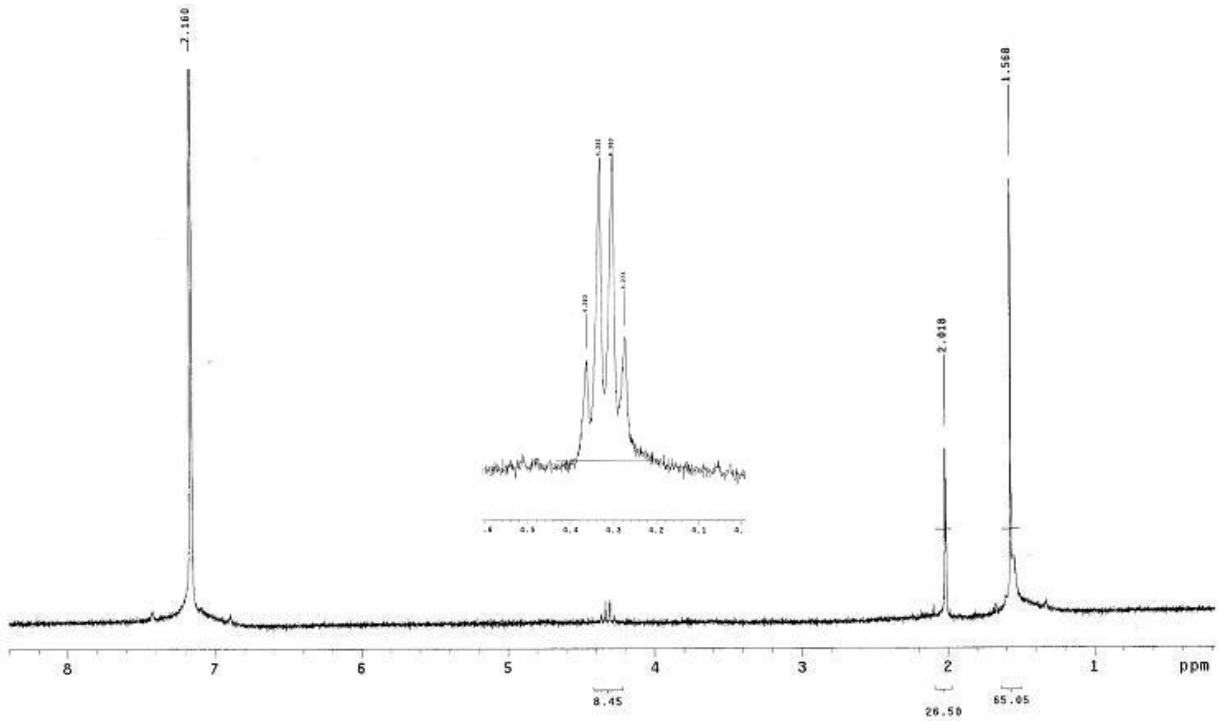

Figure SI-32. ^{1}H NMR (C_6D_6) spectrum of $Ttz^{Ph,Me}ZnOCH_2CF_3$ (**2**)

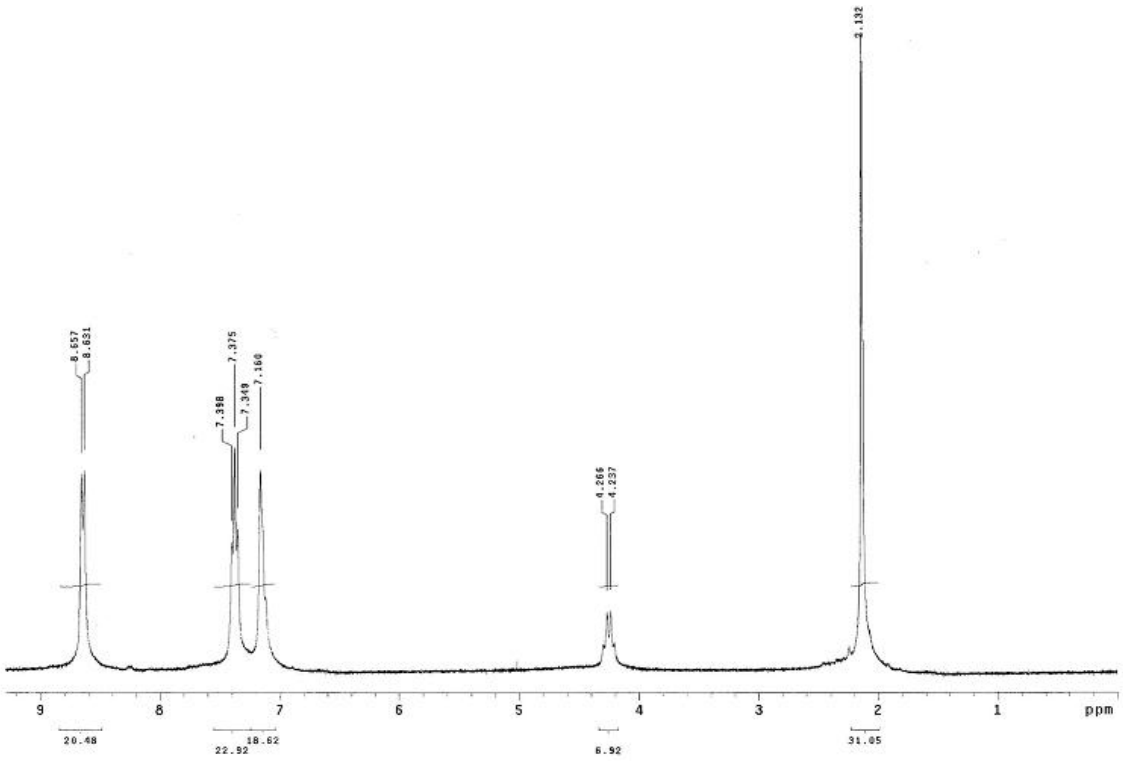

Figure SI-33. ^{1}H NMR (C_6D_6) spectrum of $Ttz^{tBu,Me}ZnOCH(CF_3)_2$ (**3**)

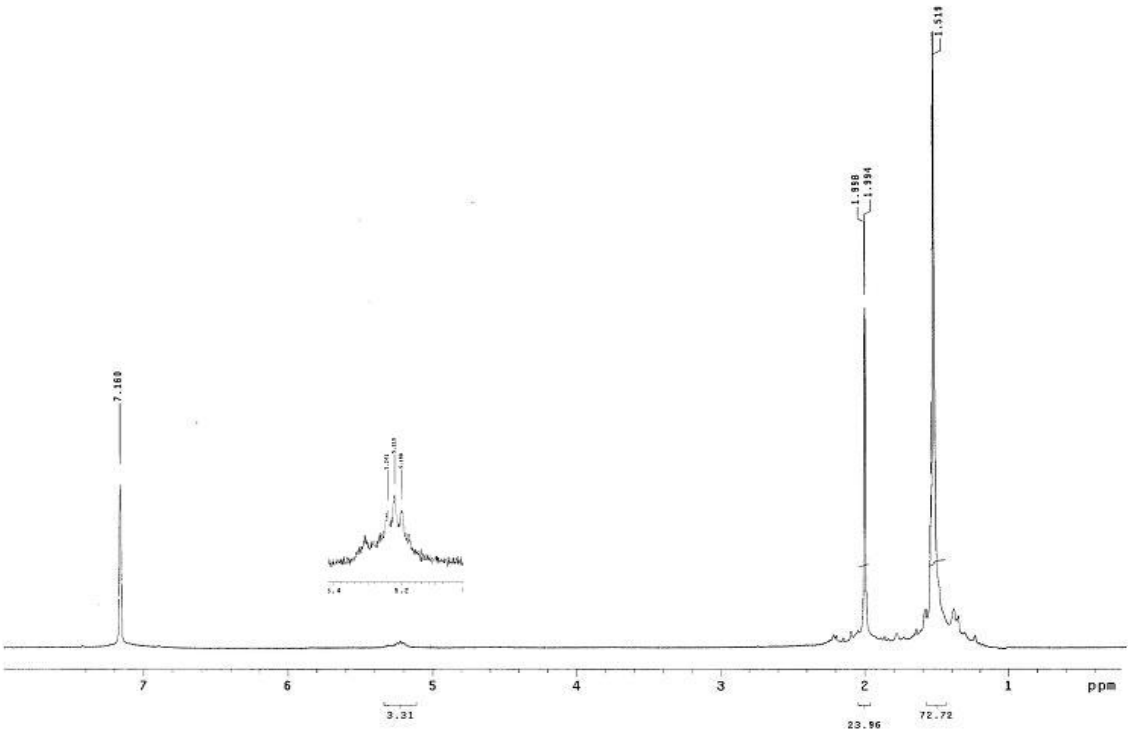

Figure SI-34. ^{1}H NMR (C_6D_6) spectrum of $Ttz^{Ph,Me}ZnOCH(CF_3)_2$ (**4**)

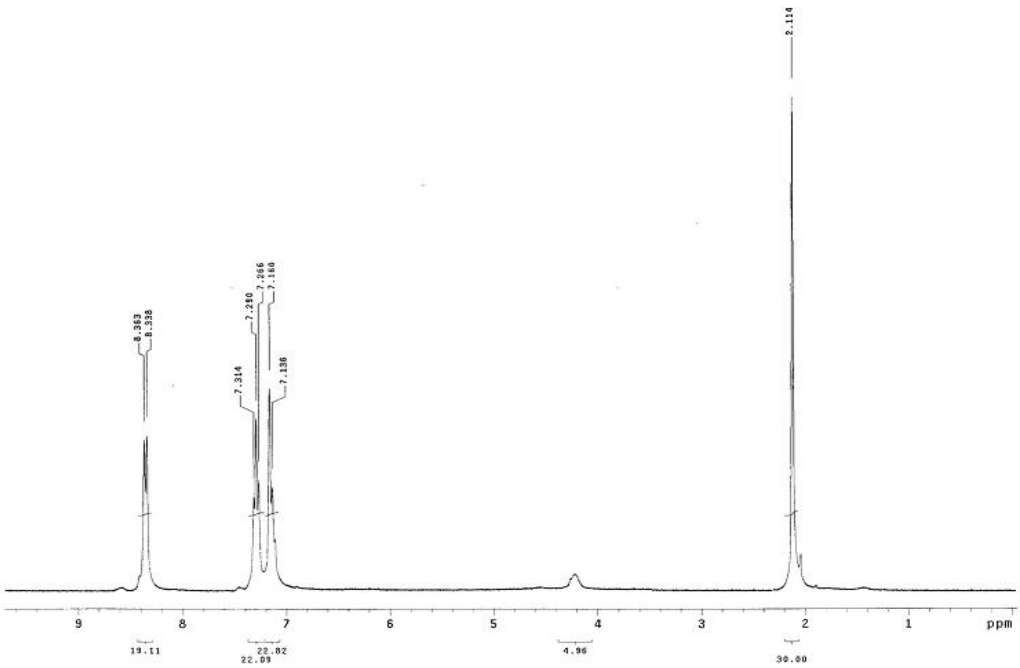

Figure SI-35. ^{1}H NMR (C_6D_6) spectrum of $Ttz^{tBu,Me}ZnOPh$ (**5**)

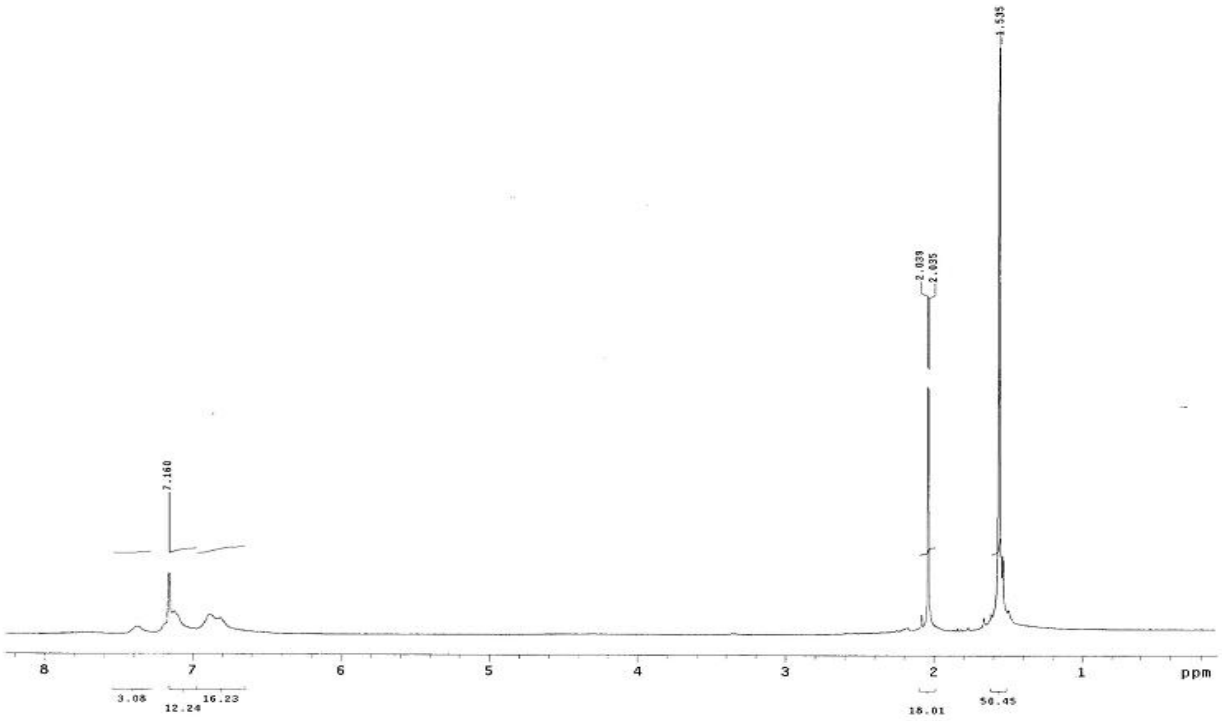

Figure SI-36. ^{1}H NMR (C_6D_6) spectrum of $Ttz^{Ph,Me}ZnOPh$ (**6**)

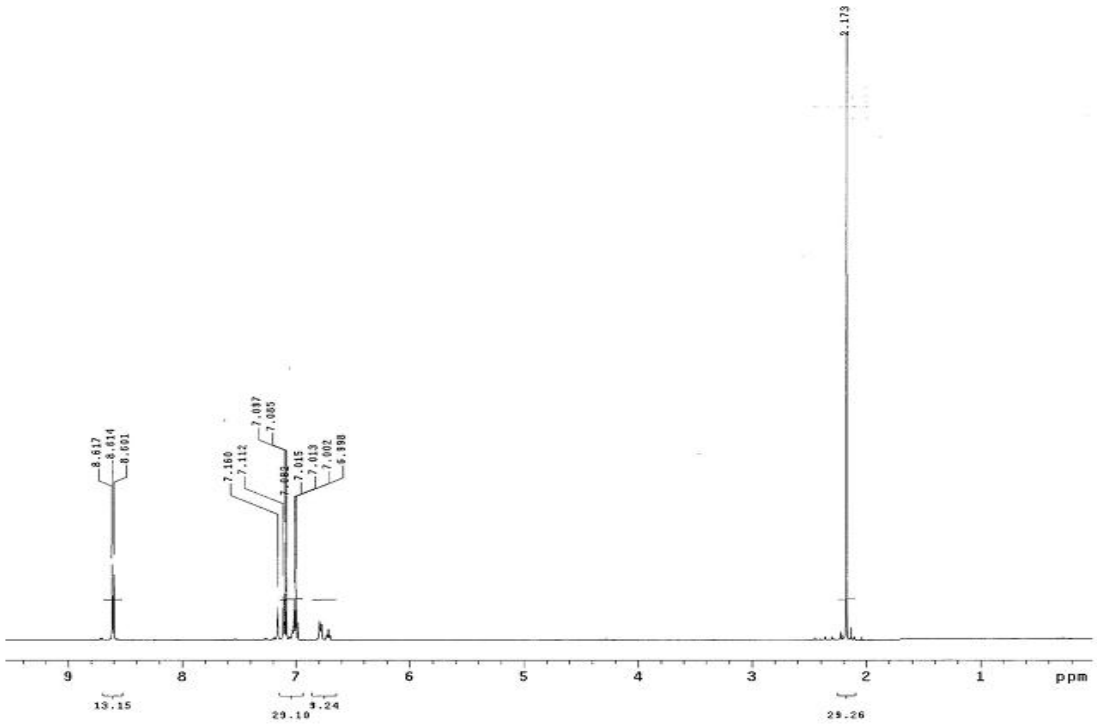

Figure SI-37. ^{1}H NMR (C_6D_6) spectrum of $Ttz^{tBu,Me*}ZnSPh$ (**7**)

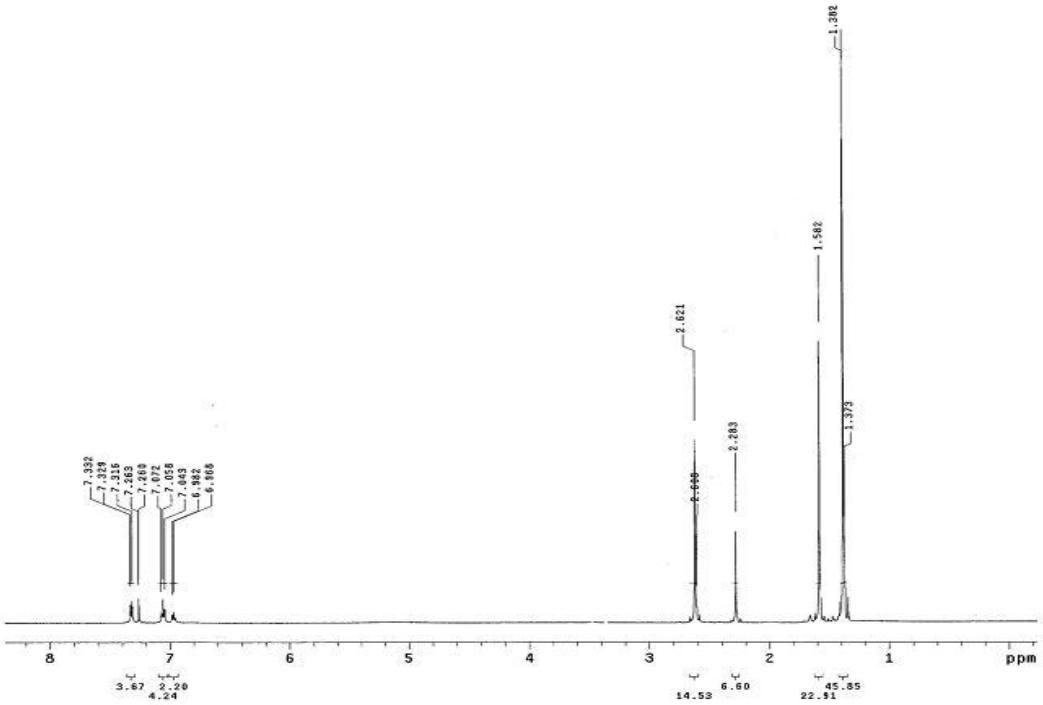

Figure SI-38. ^{1}H NMR (C_6D_6) spectrum of Ttz^{Ph,Me}ZnSPh (**8**)

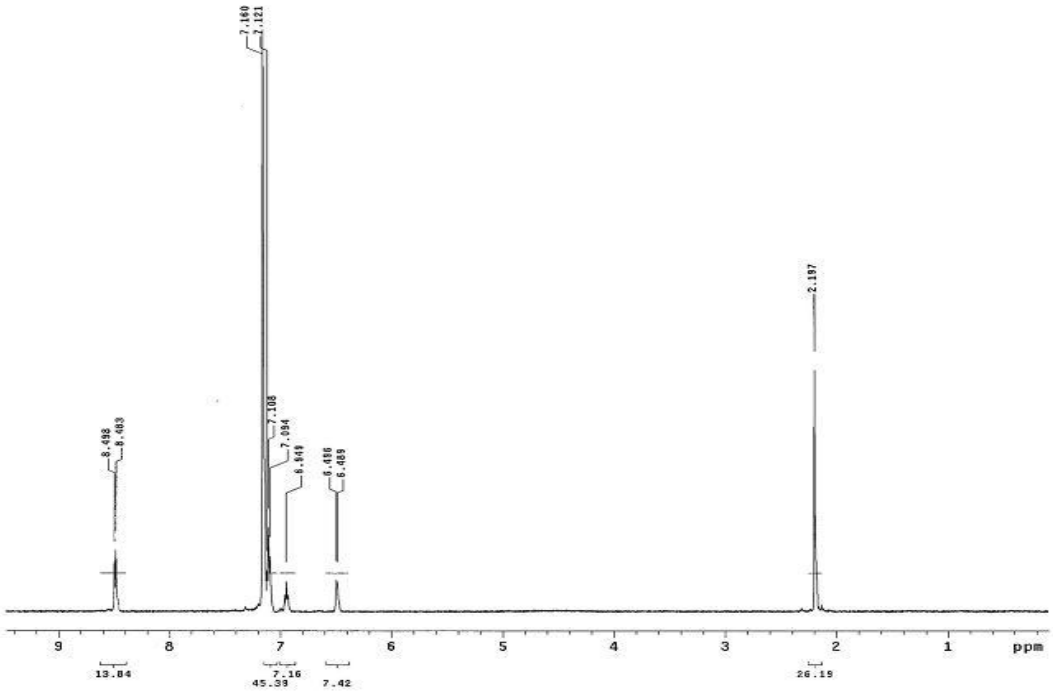

Figure SI-39. ^{1}H NMR (C_6D_6) spectrum of Ttz^{tBu,Me}Zn(*p*-$OC_6H_4(NO_2)$) (**9**)

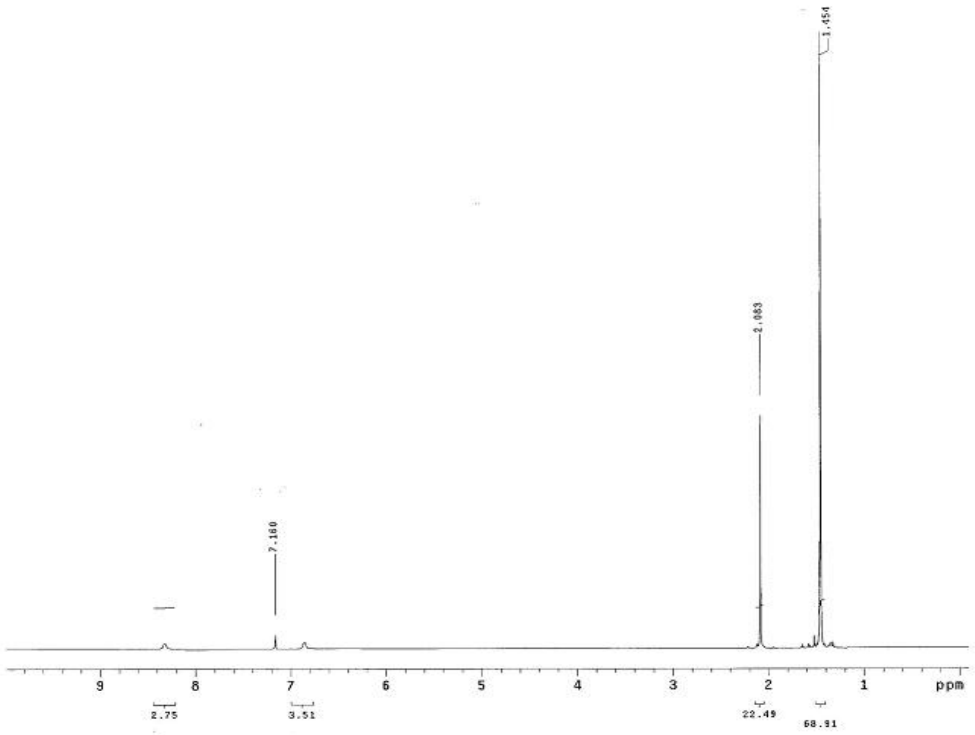

Figure SI-40. ^{1}H NMR (C_6D_6) spectrum of $Ttz^{Ph,Me}Zn(p\text{-}OC_6H_4(NO_2))$ (**10cp**)

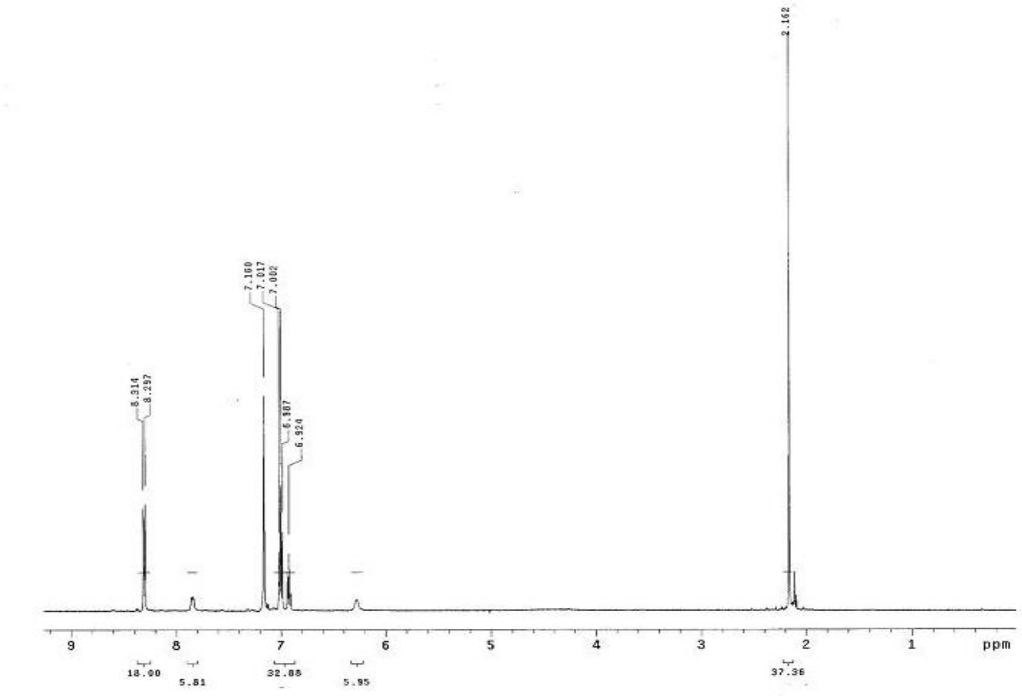

Figure SI-41. ^{1}H NMR (C_6D_6) spectrum of $Ttz^{tBu,Me}Zn(acac)$ (**11**)

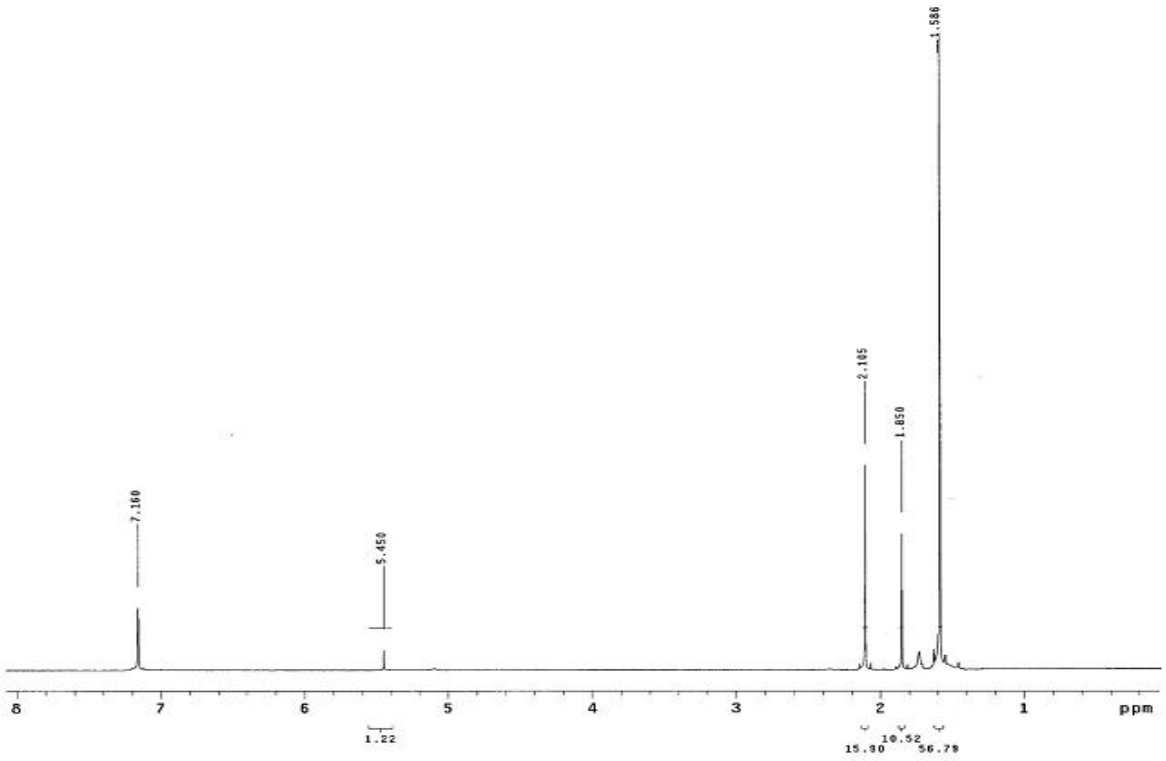

Figure SI-42. ^{1}H NMR (C_6D_6) spectrum of $Ttz^{Ph,Me}Zn(acac)$ (**12**)

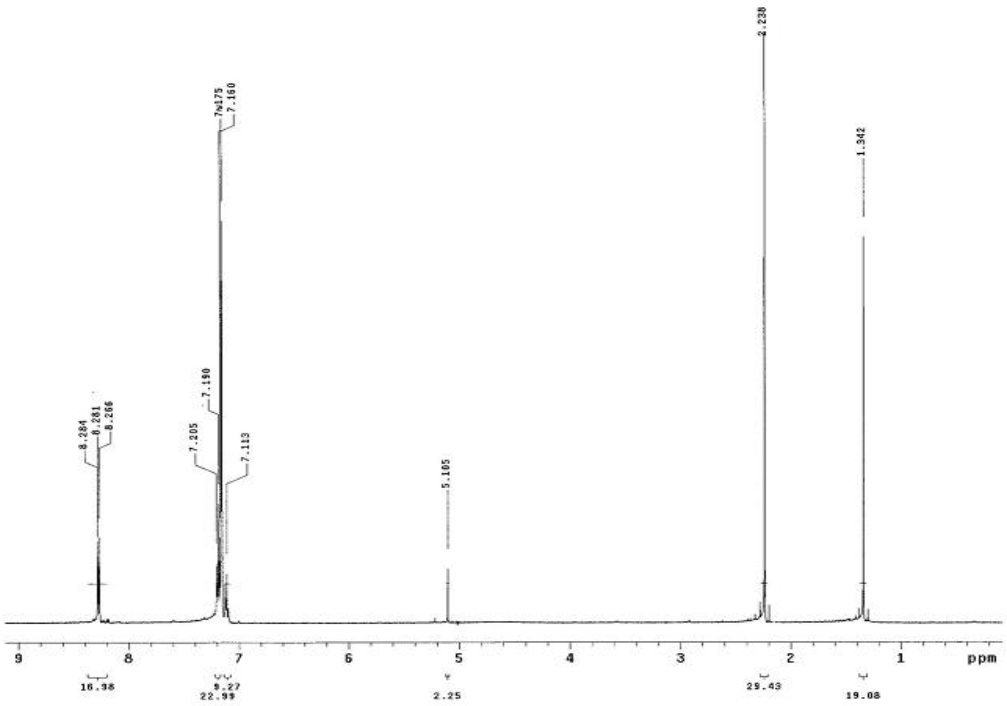

Figure SI-44. ^{1}H NMR (C_6D_6) spectrum of $Ttz^{Ph,Me}ZnOAc$ (**14**)

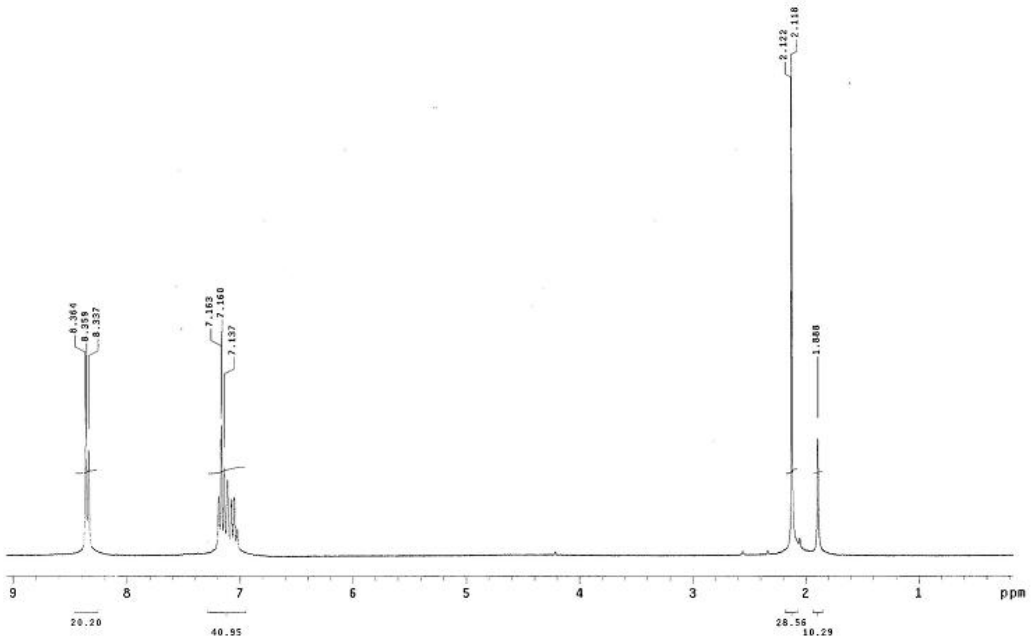

Figure SI-43. ^{1}H NMR (CD_3OD) spectrum of $Ttz^{tBu,Me}ZnOSO_2CF_3$(**16**)

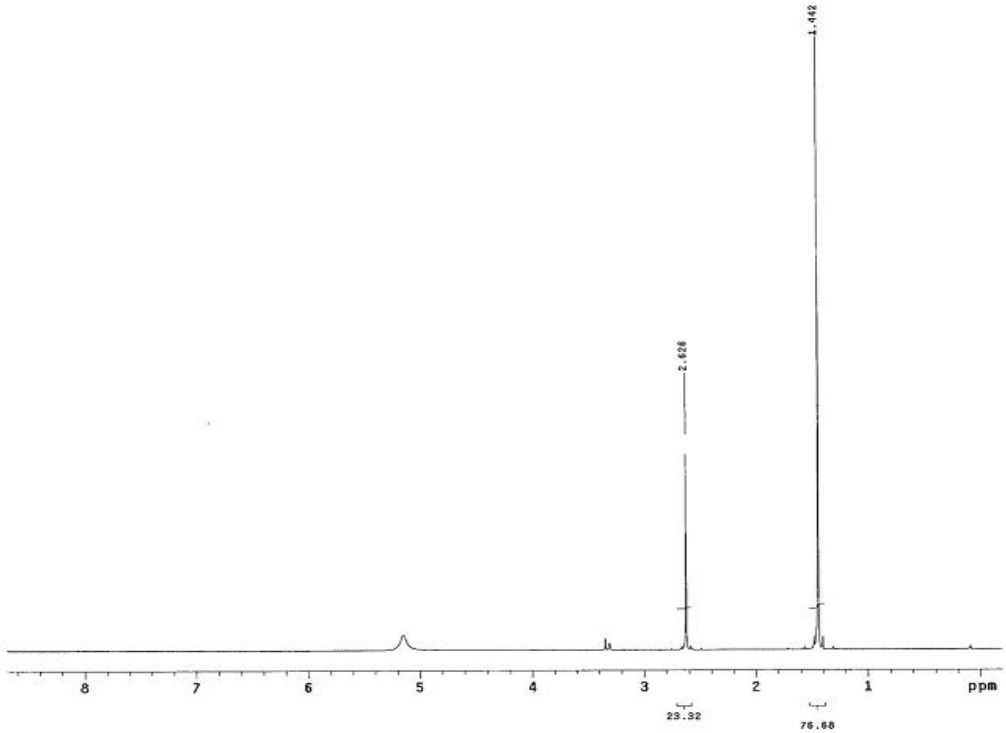

References

[1] Sluis & Spek, *Acta Cryst.* **1990**,*A46*, 194-201
[2] (a) A.L.Spek (2010) PLATON, A Multipurpose Crystallographic Tool, Utrecht University, Utrecht, The Netherlands. (b) A.L.Spek, J.Appl.Cryst. 2003, 36, 7-13. (c) A.L.Spek, Acta Cryst. 2009, D65, 148-155.
[3] G. M. Sheldrick, G. M, CELL NOW, program for unit cell determination, University of Göttingen, Germany, 2005 & Bruker AXS Inc, Madison (WI), USA, 2005.
[4] G. M. Sheldrick, Twinabs, Bruker AXS scaling for twinned crystals, version 2007/3, & Sadabs, Bruker AXS area detector scaling and absorption correction, version 2007/2, University of Göttingen, Germany, 2007 & Bruker AXS Inc, Madison (WI), USA, 2007.
[5] A. L. Spek, Platon, A Multipurpose Crystallographic Tool, 40M-Version: 40607, 1980-2007.
[6] Bruker (2005). CELL NOW, program for unit cell determination, Bruker AXS Inc, Madison (WI), USA, 2005.
[7] Bruker (2008). TWINABS 2008/2. Bruker AXS Inc, Madison (WI), USA.
[8] M. Kumar, E. T. Papish, M. Zeller, *Acta Cryst. Sect. C*., 2010, **C66**, m197-m200.
[9] C. Bergquist, H. Storrie, L. Koutcher, B. M. Bridgewater, R. A. Friesner and G. Parkin, *J. Am. Chem. Soc.* 2000, **122***,* 12651-12658.